Doctoral Dissertations and Master's Theses

Spring 5-2016

Real-Time Optimization Based Power Flow Controller for Energy Consumption and Emissions Reduction in a Parallel HEV

Abdulla Abdulaziz Karmustaji
Embry-Riddle Aeronautical University

Follow this and additional works at: https://commons.erau.edu/edt

Part of the Mechanical Engineering Commons

REAL-TIME OPTIMIZATION BASED POWER FLOW CONTROLLER FOR
ENERGY CONSUMPTION AND EMISSIONS REDUCTION IN A PARALLEL HEV

by

Abdulla Abdulaziz Karmustaji

A Thesis Submitted to the College of Engineering Department of Mechanical
Engineering in Partial Fulfillment of the Requirements for the Degree of
Master of Science in Mechanical Engineering

Embry-Riddle Aeronautical University
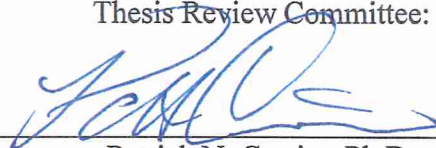Daytona Beach, Florida
May 2016

REAL-TIME OPTIMIZATION BASED POWER FLOW CONTROLLER FOR ENERGY CONSUMPTION AND EMISSIONS REDUCTION IN A PARALLEL HEV
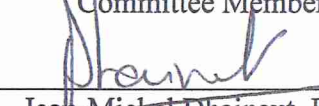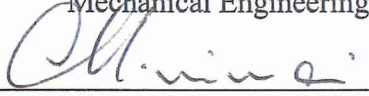
by

Abdulla Abdulaziz Karmustaji

This thesis was prepared under the direction of the candidate's Thesis Committee Chair, Dr. Patrick N. Currier, Professor, Daytona Beach Campus, and Thesis Committee Members Dr. Marc D. Compere, Professor, Daytona Beach Campus, and Dr. Ilteris, Demirkiran, Professor, Daytona Beach Campus, and has been approved by the Thesis Committee. It was submitted to the Department of Mechanical Engineering in partial fulfillment of the requirements for the degree of Master of Science in Mechanical Engineering

Thesis Review Committee:
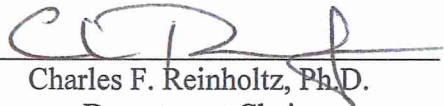
_____
Patrick N. Currier, Ph.D.
Committee Chair

_____
Marc D. Compere, Ph.D.
Committee Member

_____
Jean-Michel Dhainaut, Ph.D.
Graduate Program Chair,
Mechanical Engineering

_____
Maj Mirmirani, Ph.D.
Dean, College of Engineering

_____
Ilteris, Demirkiran, Ph.D.
Committee Member

_____
Charles F. Reinholtz, Ph.D.
Department Chair,
Mechanical Engineering

_____
Christopher Grant, Ph.D.
Associate Vice President of Academics

04/20/2016
Date

i

Acknowledgements

First of all, I would like to thank God for all the blessings, patience, and power that he gave me to achieve my goals throughout this study. God has surrounded me with people who always look out for me, given me family and friends who bless me every day which they all contributed to this work.

Secondly I would like to thank my family for always believing in me and keeping me motivated, without their prayers I could have never reached the place I am today.

Third, I would like to express the deepest appreciation to my committee chair, Dr. Currier, whose expertise, understanding, generous guidance and support made it possible for me to be proud of the work I have done. Without his help through the unexpected meetings during the days and nights for more than a year, I would have never finished this work successfully.

Fourth, special thanks to my thesis committee, Dr. Compere and Dr. Demirkiran, for all the motivation, support, and advices they provided me throughout the research. Their true opinion and comments about my work helped me to improve and be better prepared for my next chapters in my life.

Finally, I want to thank my friend Rohit Gulati for believing in me, and the time he dedicated to help me with my thesis whenever I asked for it.

Abstract

Researcher: Abdulla A. Karmustaji

Title: Real-Time Optimization Based Power Flow Controller For Energy Consumption And Emissions Reduction In A Parallel HEV

Institution: Embry-Riddle Aeronautical University

Degree: Master of Science in Mechanical Engineering

Year: 2016

As the regulations on the fuel economy and emissions standards become higher, Hybrid Electric Vehicles (HEV) are gaining more popularity in the market. HEVs improvements in fuel economy and emissions strongly depend on the energy management strategy. An optimization based power flow controller is presented in this thesis to find the appropriate power split between the Internal Combustion Engine (ICE) and the electric motor to reduce the energy consumption and emissions. However, emissions were not taken into consideration in results due to lack of reliable results. A basic power flow controller was built to compare to the optimization based controller. A plant model of each component of the vehicle was built in Simulink to evaluate the performance of each controller. Compared to the basic power flow controller, the real-time energy and emission minimization controller using shift schedule (ReTEEM-SS) reduced the energy consumption by approximately 6.2% in city driving style and 5.4% in highway driving style. The optimization based controller was further modified to replace the shift schedule with a shift logic. The real-time energy and emission minimization controller using shift logic (ReTEEM-SL) reduced the energy consumption by 10.2% in city drive style and 5.3% in highway driver style, when compared to the basic controller.

Table of Contents

List of Tables

List of Figures

Chapter I

Introduction

1.1   Background and Motivation

Climate change, air quality, and energy security are prominent and global

issues today. Government and non-governmental organizations are working to

develop new regulations and funding research to find how to tackle these issues. A

major contributor of greenhouse gas and particulate emissions is the automobile

sector, which has traditionally also been one of the largest consumers of fossil fuels.

Thus, to overcome the current environmental issues, newer, more efficient, and

cleaner technologies are being developed for implementation in cars.

A variety of options are under development, some of which augment

traditional internal combustion engines with other energy generation devices and

alternative fuel sources, while others utilize novel power generators and strictly

renewable energy sources. Nowadays, internal combustion engine (ICE) has been

used with different alternative fuel sources such as E85 and B20. E85 is made from

the ultimate renewable resource, corn, and consists of a blend of 85% ethanol and

just 15% gasoline. A flexible fuel vehicle (FFV) is specially designed to run on any

ethanol blend up to 85% ethanol, where the computer adjusts the fuel injection and

ignition timing appropriately. The main benefits of FFV is the increased power and

acceleration and reduced emissions and air pollution. However, the energy density

of E85 is less than the gasoline, as a result, it will have lower fuel economy. B20 is a

term used for 20% biodiesel, comes from renewable resources such as soybeans

and waste cooking oil, and 80% petroleum diesel to create biodiesel blend. Since it is made from renewable resources, biodiesel is better for the environment. It has higher energy density than gasoline which will result in a better fuel economy.

Another technology that has been developed to integrate with the ICE is the mild hybrid. It allows the engine to be turned off whenever the car is coasting, braking, or short stop, as well as it captures the energy from braking. This technology can be used by replacing the starter and the alternator by a single electric device to combine the purpose of both devices into one and be able to assist the power to the ICE. Furthermore, a bigger electric motor can be used to be able to operate in electric mode only, to form a full hybrid electric vehicle (HEV). Hybrid vehicles can accomplish all the benefits of mild hybrid, and operate in electric only when the battery's state of charge (SOC) is high. The battery can be charged by braking, engine or converting the heat energy from the brakes to electric energy. An electrical outlet can be used to charge the battery, such design is called a Plug-in Hybrid Electric Vehicle (PHEV). PHEVs share both characteristics of the electric vehicle (EV) and the conventional vehicle. Unlike Hybrid vehicles, EVs operate without ICE and solely depends on the wall power outlet. Another power generator device that is used in cars is fuel cell. It is considered a zero emission vehicle since it uses oxygen and compressed hydrogen, with no pollutants on the tailpipe. In addition, it has higher fuel economy than the gasoline, however, it is a very expensive technology.

Out of the many vehicle options that is available in the market, HEVs are probably the most promising and currently viable approach to reduce fuel consumption and emissions in from automobiles and reduce their environmental impact.

To encourage development of hybrid vehicle technologies, and nurture the future automotive engineers so that they enter the workforce with a motive and capabilities to produce green vehicles, Embry-Riddle Aeronautical University (ERAU) takes part in a collegiate competition called EcoCAR. EcoCAR 3 Advanced Vehicle Technology Competition, sponsored by the US Department of Energy and General Motors (GM), and managed by Argonne National Laboratory is the current and third iteration of the EcoCAR competition. Participating student teams are required to redesign the powertrain of a stock 2016 Chevrolet Camaro to turn the car into a hybrid or electric vehicle, integrating the use of alternative fuels and other innovations. Thus, teams strive to reduce the car's environmental impact while maintaining the performance and character of a muscle car. This thesis will focus on developing an energy management system for the built hybrid Camaro to distribute the torque demand from the driver to the powertrain to reduce the energy consumption and emissions.

1.2   Vehicle Architecture
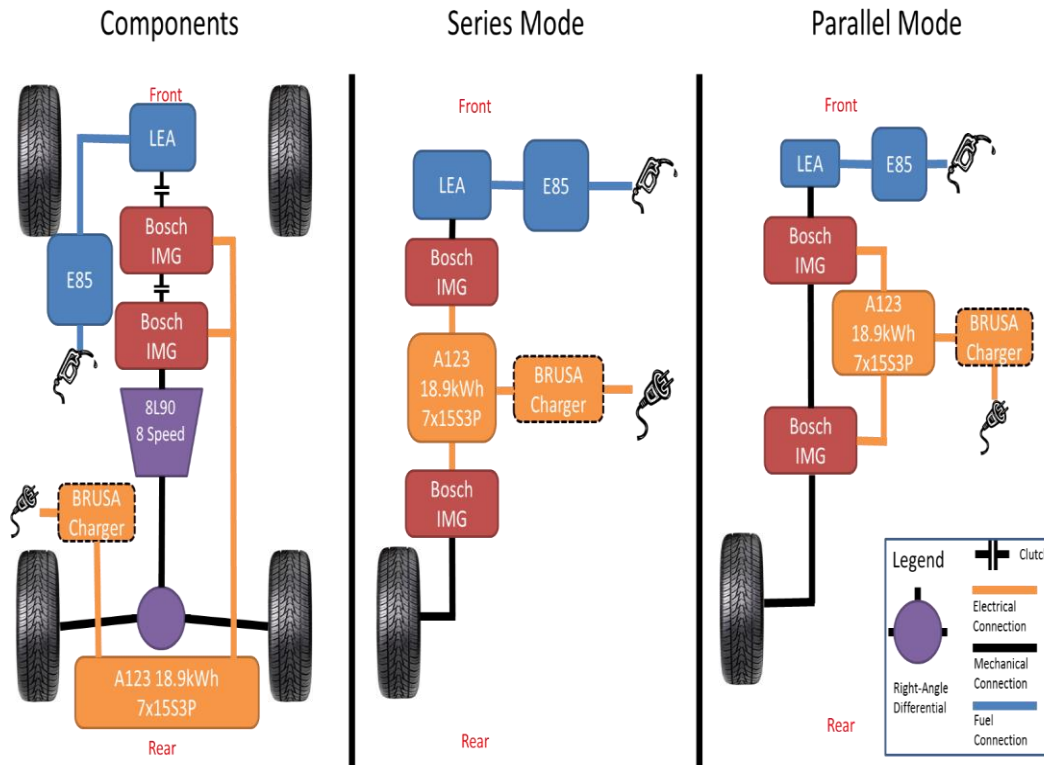
Figure 1: The component connection diagram of the vehicle architecture and the power flow in Series and Parallel operation modes.

The developed controller in this thesis is evaluated using the EcoCAR 3 Camaro HEV. The architecture that the EcoEagle team is be building is a Parallel-Series Plug-in Hybrid Electric Vehicle (PHEV), as shown Figure 1. This rear wheel drive vehicle can operate in either series or parallel hybrid configurations by engaging or disengaging the clutches. Table 1 shows the list of the components that will be added and replaced to the hybrid Camaro.

Table 1: List of the powertrain components.

Component	Manufacturer and Model	Performance specifications
Electric Traction Motor (x2)	Bosch IMG	70 kW 350 N.m
2.4L E85 ICE	GM LEA	136 kW 233 N.m
8-Speed AT Transmission	GM 8L90	--
ESS	A123 7x15sx3p	18.9 kWh

The internal combustion engine used is a donated 2.4L GM LEA ECOTec calibrated for E85 fuel. Its power is supplemented by a pair of Bosch IMG motors/generators. The motors are controlled by Bosch inverters. Tractive force is sent to the wheels through a GM 8L90 8-speed automatic transmission. The on-board energy storage system (ESS) is an A123 7x15s3p battery pack with a capacity of 18.9kWh and peak power of 177kW.

1.3   Statement of Problem and Thesis Scope

One of the challenges for the development of Parallel architecture HEVs is the energy management system (EMS) that coordinates the contributions of multiple energy sources. The main objectives of the EMS in HEVs are to increase the overall powertrain efficiency and reduce emissions while sustaining the battery charge and meeting the driver's demand for traction power. Another challenging task is to determine the gear shifting strategy for Parallel HEVs because the throttle pedal position requests a torque from the drivetrain which could come from either one or both of the mechanical power generating devices. Therefore the transmission shift points cannot primarily depend on the throttle position and the engine torque, as it

does in a conventional vehicle. The scope of the thesis is to develop a real-time

power flow controller that will optimize the operating point based on energy

consumption and emissions to handle the mentioned challenges. Emissions were

not taken into consideration in results due to lack of reliable data, but the controller

methodology section explains how it would handle the emissions if sufficient data

were available. The definition of real time is intended to convey a decision making

process that can be executed in real time while driving. The algorithm presented

relies on information available during driving in a custom supervisory control

system. The application of this algorithm in a real time computing context is left for

future work.

The new power flow controller should be able to select the appropriate

torque combination between the motor and the engine and to select the appropriate

gear without a predetermined shift schedule to reduce the energy consumption and

emissions. In addition, the power flow controller should be easily modified to be

applicable to any parallel architecture with different components.

Chapter II

Review of the Relevant Literature

This chapter presents a literature survey of various energy management approaches. Section 2.1 reviews the rule based control strategy which is widely used in HEVs. Section 2.3 discusses the main idea of the optimization based dynamic programming. Section 2.4 presents different controllers and how it is integrated with Intelligent Transportation Systems (ITS) to predict future driving pattern to manage the energy more appropriately.

2.1   Rule-Based Control Strategy (RBCS)

HEVs and PHEVs primarily use rule-based control strategy (RBCS). It uses knowledge about physical systems and components, gained through experiments, and translates it to mathematical models. For example, when used to control the components generating tractive effort in a hybrid vehicle, it is mainly based on the idea of 'load-leveling'. This means that it shifts the actual ICE/motor operating point as close as possible to the optimal point of efficiency, fuel economy, or emissions at a particular speed without a prior knowledge of the driving conditions. The idea of load leveling vehicle operation strategy for energy management is used widely in many different controllers [1], [2] , [3] and [4]. Adhikari proposed an online power flow control strategy for PHEV based on the power balancing strategy, which controls the ICE within its peak-efficiency region by using the electrical system [3]. Zhao used a fuzzy logic based controller to implement a power balance strategy on an Off-road HEV to make the engine operate close to the optimal curve [5]. RB strategies can be classified as deterministic or fuzzy RBCS.

2.1.1 Deterministic RBCS

A Power follower controller is a RBCS that uses the engine as the primary source of power, and the electric motor to provide additional power when required, while sustaining the State of Charge (SOC) of the battery. However, this deterministic strategy doesn't optimize the overall efficiency and emissions [6]. Instead, it controls the operation of the power generating devices based on the vehicle speed, SOC, and driver demand. It uses only the electric motor when the vehicle speed is below a certain threshold, and uses the ICE when the vehicle speed is above the threshold. The operating point of the ICE is kept close to optimal efficiency by producing either positive or negative torque from the motor. During braking, the motor is used to capture the kinetic energy. However, when the SOC falls below the minimum threshold, the controller requests more load on the engine to replenish the battery via electric motor.

Nowadays many HEVs use this strategy to split the torque between the engine and the motor. A comparative study was performed by Ma and Kang that shows that the GM Volt and the Toyota Prius control strategies are based on a power follower control strategy [7], as well as the Honda Insight [8].

2.1.2 Fuzzy Logic Controller (FLC)

Using prior knowledge and experiments of the drivetrain operation, fuzzy logic strategies can be used to develop a controller that will seek the optimal engine-motor torque distribution [9] [10] [11] [12] [13]. In fuzzy logic language, the input and output variables are described by linguistic values such as high, medium, and

19

low. The main advantages of FLC are the ability to deal with nonlinearity, uncertainty, and adaptation, since it can be easily tuned based on the given knowledge. Real-time operation is the most reliable way of obtaining knowledge to tune the parameters, however, it requires a long time and involves high cost [14]. Another effective way is by using simulations to tune the control parameters until achieving optimal parameters for the specified operation environment.

A fuzzy-logic based torque distribution controller was implemented and tested in a real service route for a parallel hybrid electric city bus by Lee to decrease the emissions of nitrogen oxides (NOx) from the diesel engine [9]. To acquire data for the system design of the HEV, a dynamometer test was carried out where every possible torque-speed combination of the powertrain and the corresponding NOx emissions were measured. The test results showed that the diesel engine produced relatively low torque with a large amount of emissions when its rotational speed was low. Conversely, it produced relatively high torque and a small amount of emissions when its rotational speed was high. The FLC controls the diesel engine and the motor to provide sufficient torque to the vehicle with emission characteristics that meet the vehicle emission. To ensure the SOC of the battery is sustained, the on-going battery charging control using surplus power of the diesel engine is preferred when it operates at high efficiency. The proposed fuzzy-logic based can reduce NOx emissions by 20% when the powertrain is assisted by the electric motor, compared to only a diesel engine supplying tractive effort to the drivetrain.

2.2   Optimization-based Control Strategy

In optimization-based control strategies, the goal of a controller is to minimize the cost function. The cost function for an HEV may include the energy consumption and emissions. However, their formulation is based on dynamic and static mathematical models of the powertrain systems components, resulting in sensitivity to system parameter variation, system uncertainties, imprecise measurement, and noises [15].

In order to eliminate the main disadvantage of the power follower controller – its inability to optimize the overall drivetrain efficiency – Johnson et al. [16] proposed a Real Time Control Strategy (RTCS), which minimizes the energy usage and emissions through a cost function. In order to determine the ideal operating point of the vehicle's powertrain, this control strategy considers all possible engine-motor torque pairs (candidate operating points) which meet the driver's demand. Using a time-averaged speed, the controller computes the instantaneous energy consumption and emissions for candidates. Then it calculates the 'replacement energy' that would restore the battery's SOC to its initial level. This replacement energy also accounts for the inefficiencies in the energy storage system conversion process. Furthermore, other parameters such as user-and standards-based weightings are used to impact the time-averaged fuel economy and emissions performance in the overall impact function. The controller continuously selects the operating point that is the minimum of this cost function. However, this approach is not desirable for online implementation due to the expensive computations required to determine all the possible engine-motor torque pairs. Simulations were

performed to compare the results of the RTCS and a power follower controller on a parallel HEV using ADVISOR. The RTCS reduced NOx emissions by 23% and PM emissions by 13% with a drop of only 1.4% in fuel economy.

2.3 Dynamic Programming

Another strategy to minimize the fuel consumption and emissions is dynamic programming (DP) which is used widely as HEV management system [17] [18] [19]. However, this approach is not an option for real-time implementation due to computation time and requisite prior knowledge about the entire drive cycle. Despite this, DP is a valuable analytical tool that provides important advantages while developing controllers and designing the vehicle [15]. In this optimization based control strategy, the vehicle is considered as a discrete dynamic system described by state functions. This technique is used to minimize the cost function to achieve the desired goal. The computational complexity of the DP approach is its main drawback [6].

To reduce the computational burden of DP, some variables such as battery charging and discharging, and motor efficiency are usually assumed to be constant [20]. The main benefit of DP is its ability to minimize the fuel consumption and emissions by finding the optimum point at each time instant.

2.4 Predictive CS

Many types of Energy Management Systems (EMS) have been proposed to split the torque demand efficiently to reduce the emissions and improve fuel economy based on the current driving conditions. However, an appropriate

22

allocation cannot be determined based only on the current driving condition

because the battery's charge and discharge strategy depends on an entire driving

pattern from a departure point to a destination. As a result, many strategies have

been proposed to use the predicted future driving pattern, using Intelligent

Transportation Systems (ITS) in order to choose the appropriate torque distribution

strategy between the engine and the motor. As an example, Gong proposed a control

strategy that uses on-board geographical information systems (GIS), global

positioning systems (GPS), and advanced traffic flow modeling techniques to gather

information about the future driving path and conditions [21]. Using the historic

traffic information to model driving cycles, optimal power management of PHEV is

used in the charge depletion mode, and dynamic programming algorithm is applied

to reinforce the charge depletion control such that the SOC drops to a specific

terminal value at the final time of the cycle. This proposed EMS was compared with

basic rule-based power management and showed significant improvement in fuel

economy.

Hajimiri proposed FLC for energy management based on the future state of

the vehicle using GPS in order to improve fuel consumption, emissions and

performance [22]. Furthermore, the EMS is modified to increase the state of health

(SOH) of the battery. Simulations verified that this strategy met all the desired goals.

Ichikawa proposed a novel energy management system for HEV that utilizes

car's navigation system over a commuting route. He designed an efficient technique

to manage the big amounts of collected data and cluster them into appropriate

driving patterns [23]. This makes online implementation easier and more efficient

to predict the future driving patterns based on the collected data. Using the

predicted driving pattern, it determines the appropriate distribution of energy using

the characteristics of the engine and the motor to find the optimal split, making this

a combination of predictive and deterministic RBCS. Figure 2 shows the rough

distribution of output torque from the EMS.
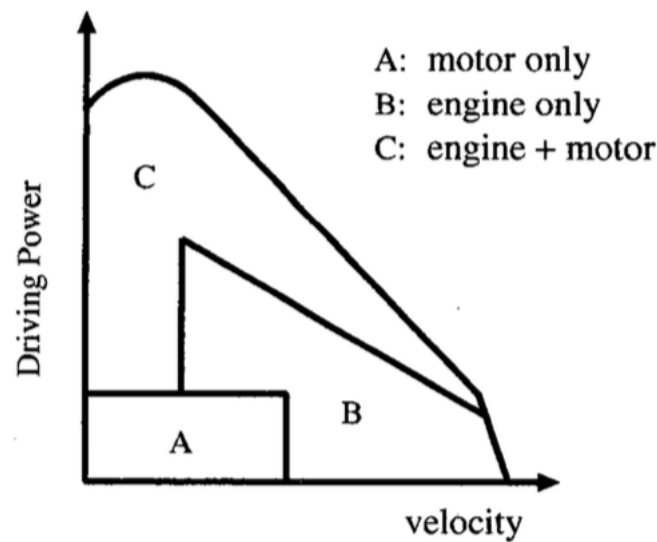
Figure 2: Engine and motor power distribution based on velocity.

Since the engine is inefficient at low loads and speeds, the motor is used to

provide the requested power. Conversely, the EMS prefers to use power from the

engine at higher vehicle speeds. However, to sustain the battery's SOC, the

distribution can vary so that the surplus power from the engine can be captured in

the ESS.

Chapter III

Methodology

The purpose of the power flow controller is to demand the appropriate torque distribution between the electric motor and the ICE that will correspond to the appropriate operating point to reduce the energy consumption and/or emissions while meeting the desired road load from the driver.

3.1   Vehicle System Modeling

Simulink and Matlab were used as a modeling environment to simulate the behavior and evaluate the performance of parallel-series PHEV. Matlab scripts were created that contained all relevant vehicle parameters to be used by the plant models for different components, as well as the drive cycles as input to the main model in Simulink. The drive cycle script reads an excel spreadsheet, consisting of two column matrices, in which the first column represents time in seconds and the second column represents the corresponding desired vehicle speed in miles per hour. Figure 3, Figure 4, Figure 5, and Figure 6 show all the four drive cycles used to evaluate the performance of the vehicle, obtained from United States Environmental Protection Agency (EPA) website [24]. The 505 drive cycle, as shown in Figure 3, is the first 505 seconds of the Urban Dynamometer Driving Schedule (UDDS). Since US06 city and highway drive cycles are short, they are repeated to ensure the ability of the controller to sustain the charge of the battery.
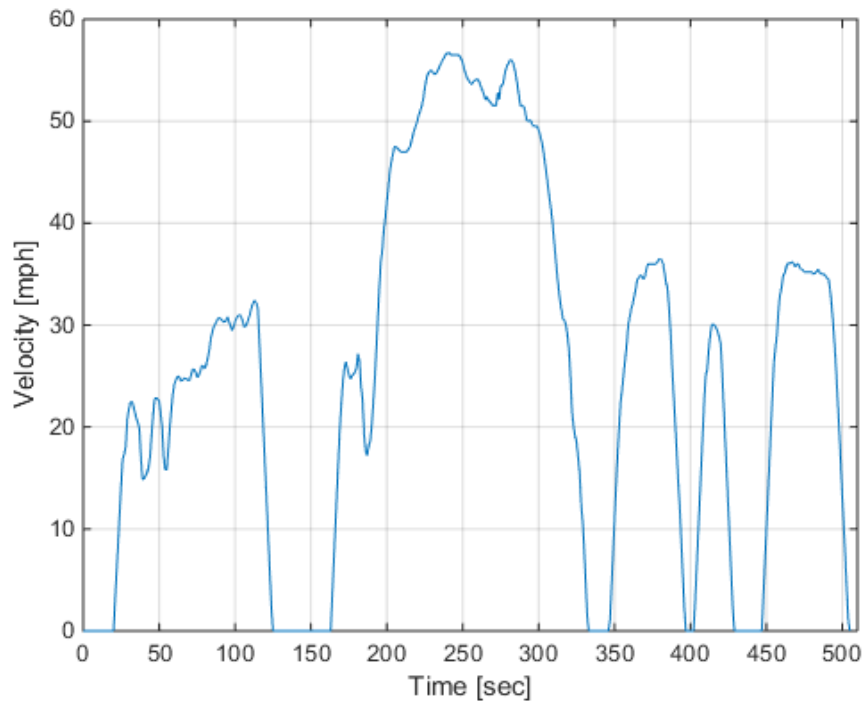
Figure 3: 505 Drive cycle to mimic low speed drive style.
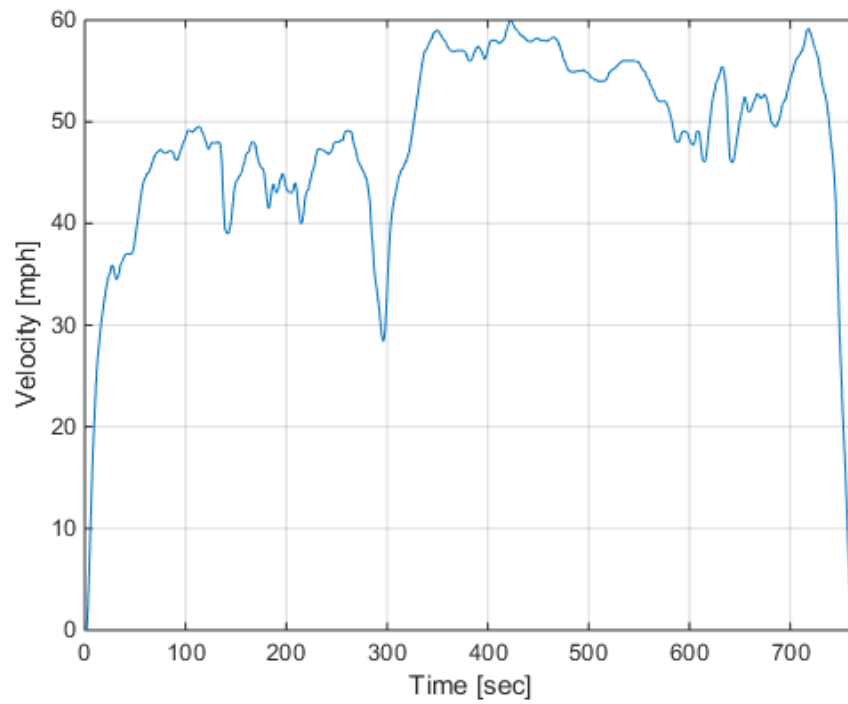
Figure 4: Highway Federal Economy Test (HWFET) to mimic high speed
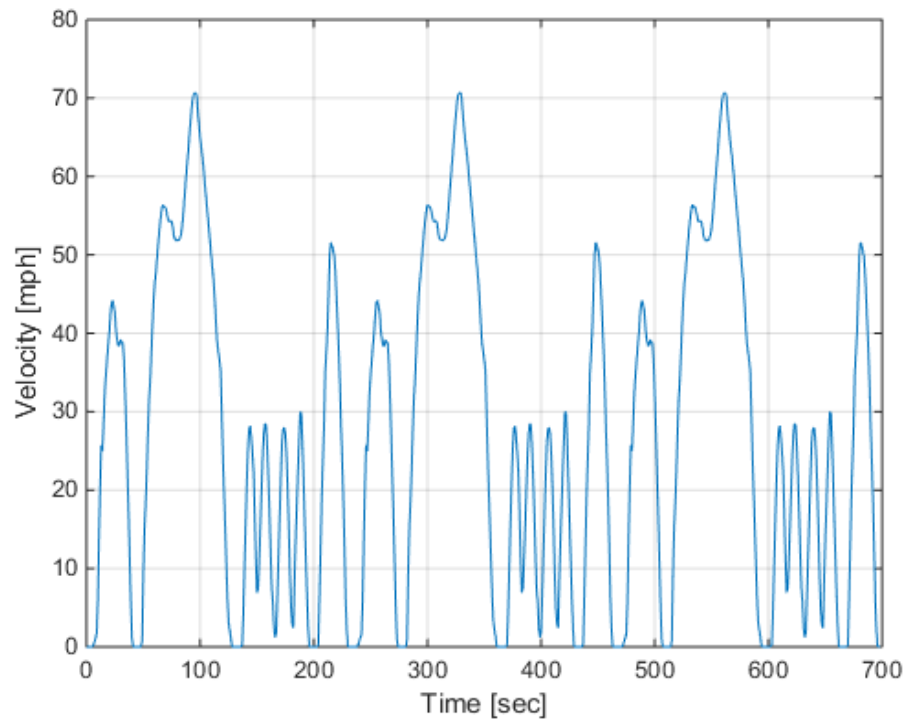
Figure 5: US06 City drive cycle to mimic aggressive low speed drive style.
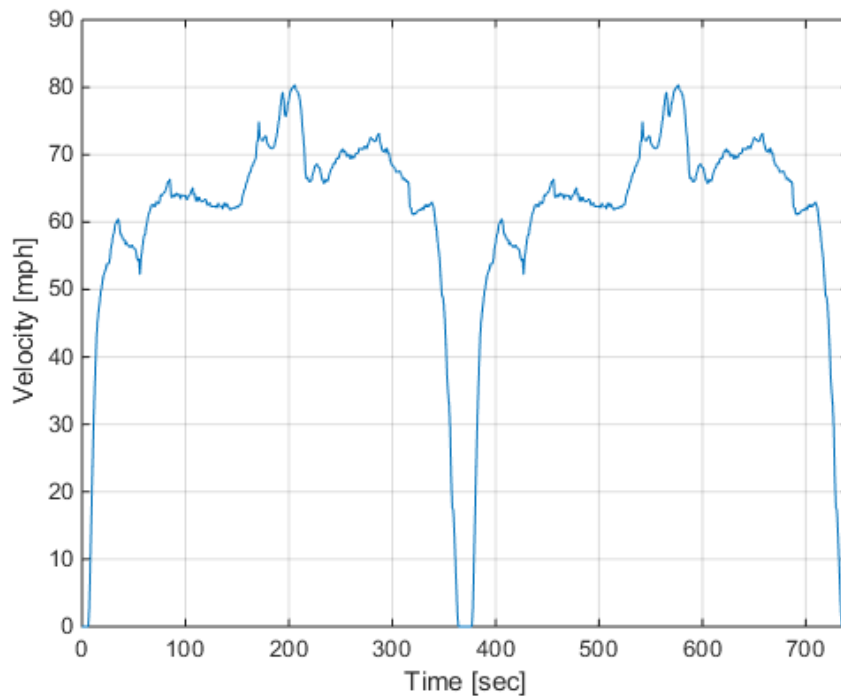
Figure 6: US06H drive cycle to mimic aggressive high speed.

27

Starting from the top level in Simulink, as shown in Figure 7, the four main

subsystems are the Driver, Power Flow Controller, Powertrain, and Glider.
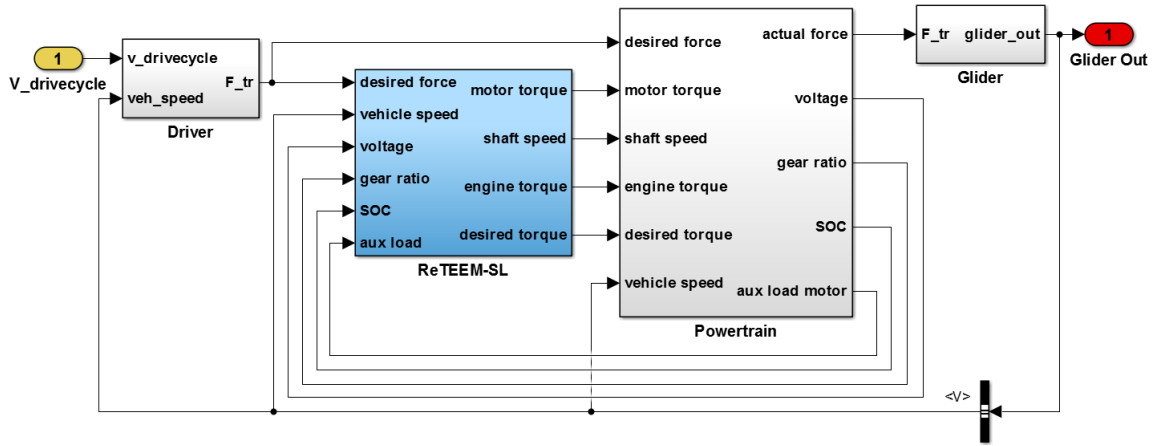
Figure 7: The top model in Simulink

3.1.1 Driver

The Driver subsystem generates the desired tractive force to the powertrain

based on the drive cycles speed and vehicle speed. This is done by using a PID

controller to find the appropriate overall tractive effort in order for the vehicle to

follow the drive cycle which is based on the difference between the desired and

actual vehicle speed. The tractive effort is then fed into the Powertrain subsystem

that contains all the plant models of the vehicle's components.

3.1.2 Powertrain

In HEVs, the desired torque from the driver needs to be distributed

efficiently between the motor and engine. Three different power flow controllers

will be evaluated and explained in more detail. The output of the controller is a

demand electric motor and engine torque from the powertrain.

28

3.1.2.1   Internal Combustion Engine (ICE)

The ICE block models the characteristics of the GM LEA engine as given in Table 2.

Table 2: Characteristics of the modeled engine.

Characteristic	Value
Displacement	2384 cc
Cylinders	I4 VVT
Fuel	E85 DI
Maximum power	136 kW @ 6700 rpm
Maximum torque	233 Nm @ 4900 rpm

The engine speed (ω) is an input to the one-dimensional lookup table to determine a maximum available torque. The engine output torque is the minimum between the maximum available torque and the demand torque. To calculate the instantaneous and accumulated fuel consumption, the engine output torque and ω are inputted into a two-dimensional brake specific fuel consumption (BSFC) lookup table that contains fuel flow rate data (in kg/s). Equation 1 is used to find the fuel power input to the engine for further performance calculations of the energy and efficiency.

$$P_{fuel}[W] = inst.fuel.rate \left[\frac{kg}{s}\right] \times \rho_{fuel\,energy} \left[\frac{KWh}{kg}\right] \times 3600 \left[\frac{s}{h}\right] \times 10^3 \left[\frac{1000\,W}{1\,kW}\right] \quad (1)$$

Engine braking and thermal effects are not considered and will not change the performance of the engine. The operating range is restricted between the idling speed of 600 rpm and the redline speed of 6500 rpm using Saturation blocks. The accessory loads are accurately taken into consideration since the experimental BSFC

data used accounts for the mechanical coolant pump and oil pump running off the crankshaft, leading to a slightly higher fuel flow rate.

3.1.2.2 Electric Motor

The Motor model uses torque characteristics of the 70 kilowatt Bosch IMG motors which was obtained from the manufacture, however, it is not shown because the data is proprietary.

The bus voltage along with the shaft speed are inputs to the two-dimensional torque look-up tables to find the maximum motoring and regenerative braking available torques. The motor output is the minimum between the maximum available torque and the desired torque. The output torque and the through shaft speed are used to calculate the operating efficiency through two-dimensional lookup tables for both motoring and regenerative braking. The motor efficiency is used to calculate either an increased current demand from the ESS or a decreased regenerative current sent to the ESS. Due to a lack of manufacturer provided data, the performance outputs of the Motor model are affected only by the ESS provided voltage. Other effects not modeled in the Motor plant are the performance derating due to increasing operating temperature, inertia and back electromotive force (emf).

3.1.2.3 Energy Storage System (ESS)

The ESS was modeled with physics-based calculations and then parameters were optimized by testing the similar battery pack in the EcoEagles' EcoCAR 2 competition vehicle [25]. The modeled ESS is an 18.9kW-hr lithium iron phosphate battery. Its characteristics are shown in Table 3 which is obtained from [26].

Table 3: Characteristics of the evaluated battery.

Characteristic	Value
Battery Chemistry	Lithium Iron Phosphate
Battery Pack	7x15sx3p
Cell Capacity (minimum)	19.6 Amp-hr
Cell Voltage (nominal)	3.24 volts
Pack Voltage (nominal)	340 volts
Pack Energy (minimum)	18.9 kW-hr

For parameter optimization, two tests were performed – constant and variable current discharge. For both tests, the voltage was measured to be compared with the model voltage as shown in Figure 8 and Figure 9 [26].
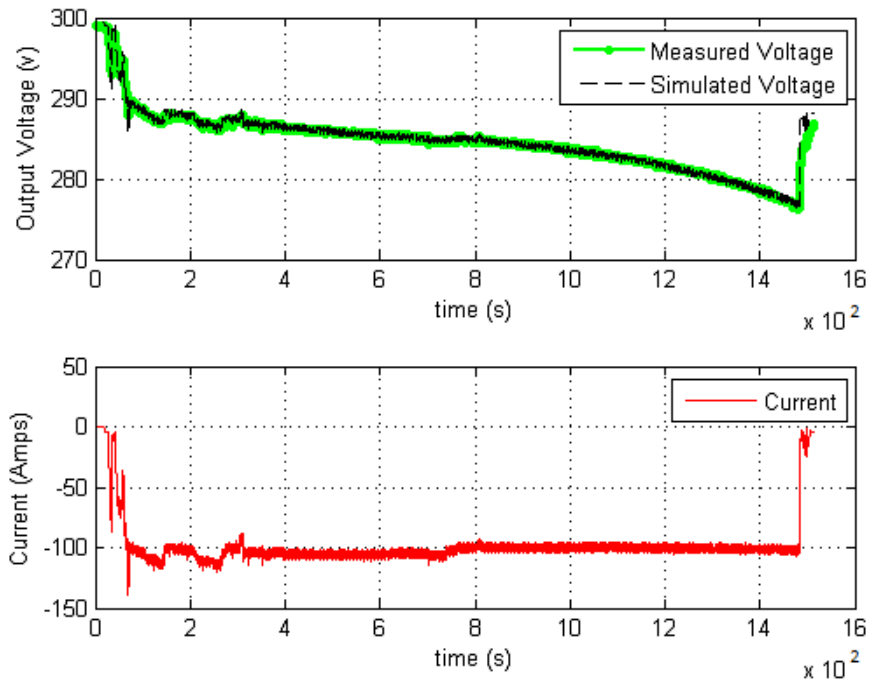
Figure 8: Measured and simulated voltage for a constant discharge current of 100 Amps.
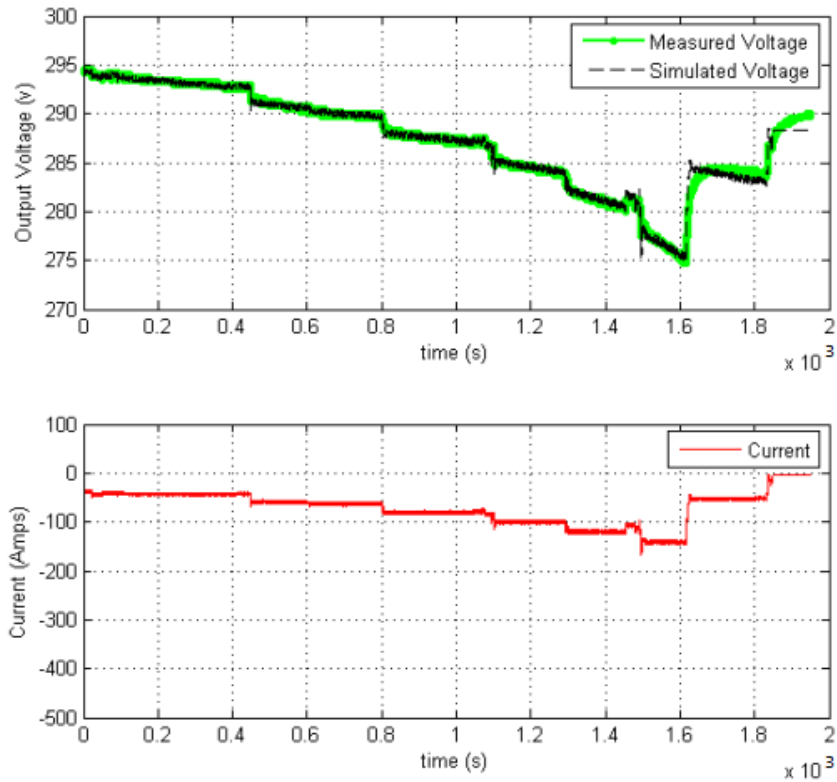
Figure 9: Measured and simulated voltage for a variable discharge current.

The mean squared errors between measured and simulated data for constant and variable discharge tests are 0.26 and 0.21 volts, respectively. This validates the ESS model developed. See [26] for full detail of the ESS modeling process.

3.1.2.4   Transmission

The Transmission subsystem is modeled using the characteristics of the eight-speed automatic transmission (8L90) obtained from GM using state flow in Simulink [27]. The gear ratios used in this transmission and the final drive ratio are listed in Table 4.

Table 4: Gear reductions used on the modeled vehicle.

Gear Number	Gear Ratio
1	4.56
2	2.97
3	2.08
4	1.69
5	1.27
6	1.00
7	0.85
8	0.65
Final Drive	2.85

The eight-speed transmission controller decides when the Transmission needs to upshift, downshift or stay in the current gear based on vehicle speed thresholds calculated as shown in Figure 10. The throttle and vehicle speed are inputted to the two-dimensional lookup tables to obtain the corresponding gear shift speed threshold. The up-shift and down-shift maps were obtained from GM but are not shown because they are proprietary.
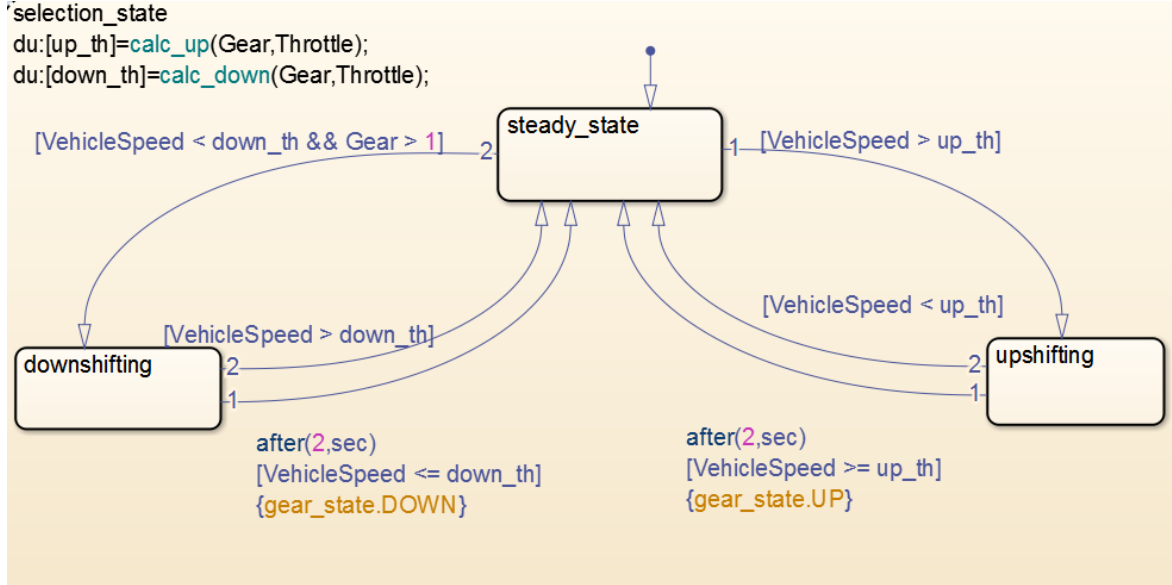
Figure 10: Transmission controller using shift schedule.

Since most of the simulations were run in charge sustain mode, which is mainly based on the ICE, the throttle calculation was based only on the ICE as shown in equation 2.

$$throttle\ [\%] = \frac{\tau_{engine,output}}{\tau_{engine,max}} \tag{2}$$

The gear number from the transmission controller state flow block is fed to the one-dimensional look-up table to find the corresponding gear ratio. The combined torque from the Motor and the ICE is then multiplied by the gear ratio, and the shaft speed is divided by the ratio, to form the output torque and shaft speed from the transmission, as shown in the Equations 3 and 4

$$\tau_{post-transmission} = GR \times \tau_{pre-transmission} \tag{3}$$

$$\omega_{post-transmission} = \frac{\omega_{pre-transmission}}{GR} \tag{4}$$

34

where GR is the transmission gear ratio.

3.1.2.5 Wheels and Differential

The Differential and Wheels block is simply converting the torque output

from the transmission to the tractive effort at the wheels, as shown in Equation 5

$$F_{post-differential} = \frac{\tau_{post-transmission} \times FDR}{r_{tire}} \tag{5}$$

where the FDR is the final drive ratio. The parameter for the tire is set to the same

value as the baseline vehicle, 0.341 meters, which were provided by the competition

sponsors.

3.1.3 Glider

The Vehicle Body subsystem evaluates the effect of all the forces – tractive,

rolling, grade and aerodynamic drag – on the vehicle's speed. Equation 6 through 9

show all formulas used to calculate all forces.

$$F_{aero} = \frac{1}{2}C_D \times \rho \times A \times v^2 \tag{6}$$

where C_D is the drag coefficient, ρ is air density, and A is the frontal area.

$$F_{rolling\ resistance} = m \times g \times C_{rr} \tag{7}$$

where m is the mass of the vehicle, g is the gravity, and C_{rr} is the rolling resistance

coefficient.

$$F_{grade} = m \times g \times \sin\tan^{-1}(road\ incline[\%]) \tag{8}$$

Thus,

$$F_{road\ load} = F_{tractive} - F_{aero} - F_{rolling\ resistance} - F_{grade} \qquad (9)$$

Table 5: Vehicle parameters.

Vehicle Parameter	Value
Mass	2020 [kg]
Frontal area	2.222 [m²]
Drag coefficient	0.344
Rolling resistance	0.01
Initial velocity	0 [m/s]
Road incline	0 [%]

The parameters entered into this block are listed in Table 5. These

parameters have been updated from the stock vehicle values to reflect the physical

modifications made to the car when the new powertrain is added. The values were

obtained by building a CAD model of the vehicle in Siemens NX [25].

3.2   Power Flow Controller

For HEVs, at any time for any vehicle speed, the control strategy has to

determine the power split between energy sources. In this thesis, three power flow

controllers were developed for the same vehicle. First, a basic power flow controller

that uses the engine as a primary source of power when the vehicle is in CS mode.

Second is the optimization based power flow controller which is the main focus of

the thesis work. Third is a modified optimization based power flow controller which

substitutes the traditional shift schedule with a shift logic.

3.2.1 Basic Power Flow Controller
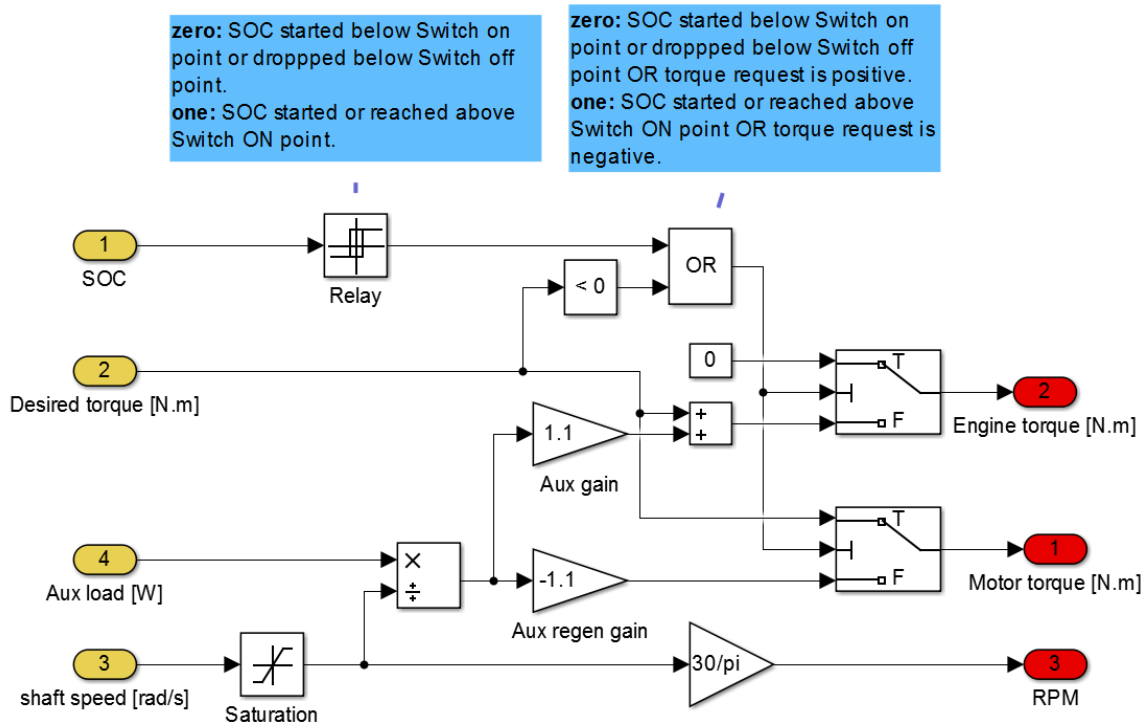
Figure 11: Simulink block diagram of the basic power flow controller.

The basic controller was developed for two main reasons. First, to have a basic running controller so the new powertrain of the new Camaro can be put together and perform bench testing until a better controller is developed. Second, to have a basic controller that the new developed controller can be compared to.

The controller demands zero torque from the engine and τ_{motor} equal to the output of equation 1 under these conditions:

    a.   The SOC is above the minimum threshold: charge deplete (CD) mode

    b. $\tau_{demand} < 0$: the vehicle is slowing down

37

Otherwise, the controller demands torque from the engine as shown in the

equation 10, and demands negative τ_{aux} from equation 11.

$$\tau_{engine/motor}[N.m] = \tau_{demand}[N.m] + \tau_{aux}[N.m] \qquad (10)$$

where the auxiliary torque is calculated using,

$$\tau_{aux}[N.m] = 1.1 \times \frac{Aux\ Load[W]}{\omega[\frac{rad}{s}]} \qquad (11)$$

The constant value of 1.1 is used to account for the average efficiency loss of

the electric motor.

3.2.2   Real-Time Energy and Emission Minimization Controller (ReTEEM-SS)

The main objective of the controller is to find the optimal split between the

engine and the motor. An optimization based controller is developed to minimize a

cost function J as shown in equation 12.

$$J = data_{norm,user\ weighted} = k_{user} \times data_{norm} \qquad (12)$$

where $data_{norm}$ is obtained by following the procedure explained in section 3.2.2.1

through section 3.2.2.8, and k_{user} is a user defined weighting that modifies the cost

function to prioritize the desired factor. The cost function J is subject to the

constraints

$$\begin{aligned} \dot{x} &= f(x,t,u) \\ g(x,u) &= 0 \\ h(x,u) &\leq \begin{bmatrix} 0 \\ 0 \end{bmatrix} \end{aligned} \qquad (13)$$

where f is the dynamical state equation, x the state variables, t the time index, u the vector of inputs, g the equality constraints and h the inequality constraints [28]. The state variables are the total energy consumption and the emissions. The equality constraint will assure that the initial and the final SOCs are equal. The inequality constraint will assure that the current SOC will not exceed the upper limit of the battery's SOC or drop below the lower limit of the batter's SOC. All of these constraints are implemented in Simulink. Figure 12 shows the main steps of this controller to minimize the cost function J.
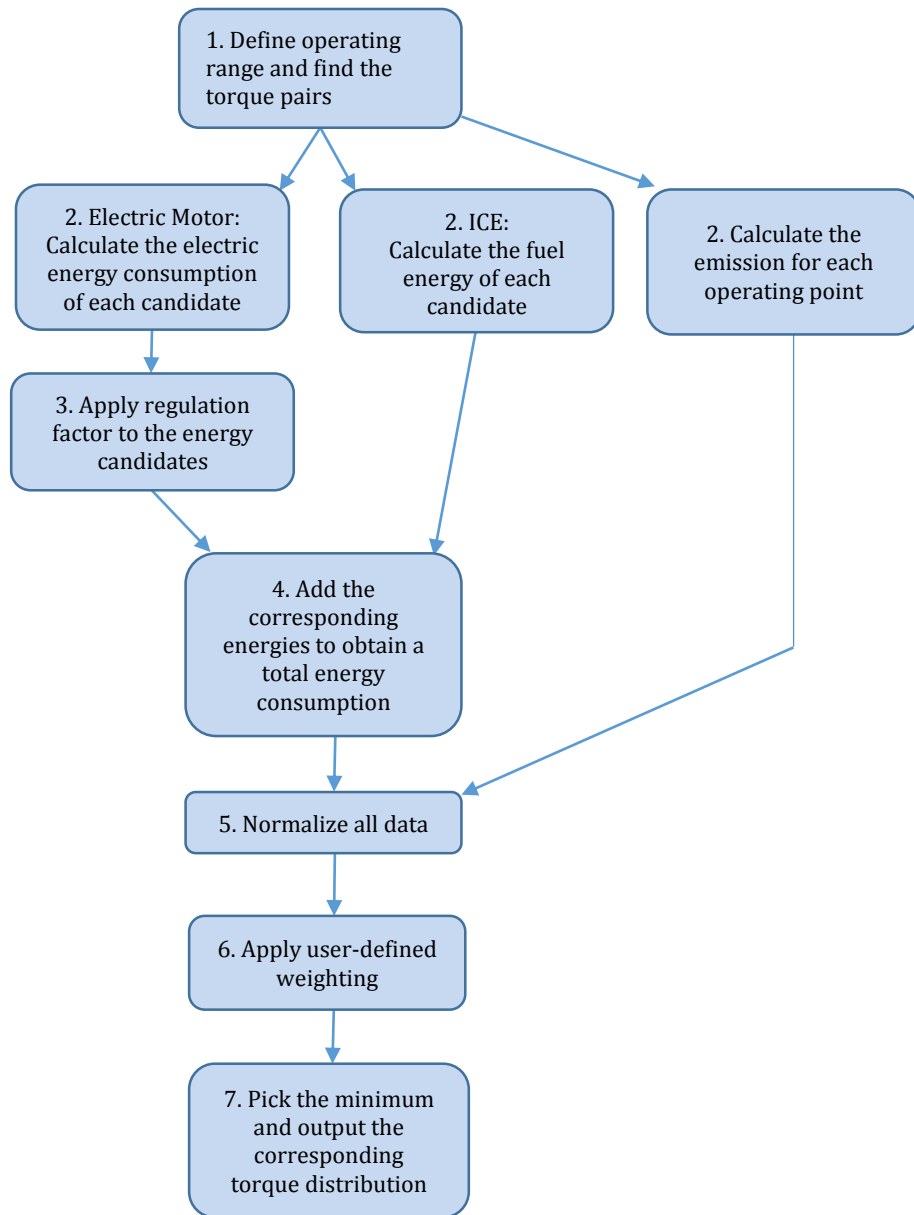
Figure 12: ReTEEM-SS controller algorithm.

First, the controller determines two vectors of torque distribution candidates between the two energy sources based on their limitations. Then it calculates the electrical and fuel energy consumption for each candidate. The electrical energy is regulated mainly based on the SOC to determine the operating mode. The sum of each torque-pair candidate energy is normalized to form a vector of normalized

total energy consumption. Based on data availability, the controller calculates a vector of the corresponding emission candidates of the each pollutant. Based on user priority, the controller outputs the optimal split to achieve the desired objective. The concept of calculating the torque distribution candidates was obtained from [16].

3.2.2.1   Motor and ICE Torque Candidates

The desired torque from the driver is split between the electric motor and the engine, and then the electrical and fuel energies are calculated. To compare the possible torque combination candidates of the motor and the engine while achieving the desired torque, the upper and lower motor torque limits are calculated at each time step. The upper limit of motor torque is

$$\tau_{motor,upper} = \min(\tau_{desired}, \tau_{motor,available}) @ \text{ current shaft speed } (\omega) \quad (14)$$

where the available torque from the motor depends on the motor and battery capabilities. The lower limit of motor torque ($\tau_{motor,lower}$) is

$$\tau_{motor,lower} = \max(\tau_{desired} - \tau_{engine,max}, \tau_{motor,max,regen}) @ \text{ current } \omega \quad (15)$$

where the maximum regenerating motor torque is also based on the motor and battery capabilities. The upper and lower motor torque limits are used as arguments for a Matlab function defined in Simulink which uses "linspace()" to generate a vector of linearly spaced motor torque candidates ($\tau_{motor,candidates}$) between the two limits. The respective engine torque candidate's vector is

$$\tau_{engine,candidates} = \tau_{motor,upper} - \tau_{motor,candidates} + \tau_{engine\ extra} \qquad (16)$$

When the electric motor alone can't supply the desired torque, extra torque is demanded from the engine candidates to get the final engine torque candidates using

$$\tau_{engine\ extra} = \tau_{desired} - \tau_{motor,upper} \qquad (17)$$

such that the total of the engine and motor torque candidates matches the desired torque. This equation is used only when the motor can't fulfil the desired torque, and outputs zero otherwise. The outputs of this step are the two vectors, $\tau_{motor,candidates}$ and $\tau_{engine,candidates}$ using n number of candidates, as shown below.

$$\tau_{motor,candidates} = [\tau_{motor,lower} \quad \tau_{motor}(2) \quad \tau_{motor}(3) \quad \dots \quad \dots \quad \tau_{motor,upper}] \quad (18)$$

$$\tau_{engine,candidates} = [(\tau_{motor,upper} - \tau_{motor,candidates}(1) +$$

$$\tau_{engine\ extra}) \quad (\tau_{motor,upper} - \tau_{motor,candidates}(2) +$$

$$\tau_{engine\ extra}) \quad \dots \quad \dots \quad (\tau_{motor,upper} - \tau_{motor,candidates}(n) + \tau_{engine\ extra})] \qquad (19)$$

Corresponding values from each index of the $\tau_{motor,candidates}$ and $\tau_{engine,candidates}$ form the candidate operating points.

3.2.2.2 Electric Energy Candidates

After obtaining the motor torque candidates, the electrical energy of each candidate needs to be calculated to form an equivalent electrical energy vector for

the controller to evaluate. The $\tau_{motor,candidates}$ at each time step and ω are input to the motor efficiency look-up table to obtain the corresponding efficiencies. To calculate the current demand from the battery, equation 20 is used.

$$I_{demand,candidates} = \frac{\tau_{motor,candidates} \times \omega}{V} \tag{20}$$

The voltage in equation 20 is obtained from the battery plant model. Then the corresponding efficiency is multiplied or divided by I_{demand} for each candidate, depending on whether the electric motor is motoring or generating, to obtain the actual current that the motor would request from the battery.

The vector of total current demand candidates $(I_{total,demand,candidates})$ is formed by adding a scalar auxiliary current to the $I_{demand,candidates}$ vector. It is then multiplied by the battery voltage to find the battery power output. The total current demand for each candidate is squared and multiplied by the battery resistance (which is a function of the SOC) to find the electric power loss from charging or discharging the battery. For each candidate, the battery power and the power loss are added to obtain the total battery power output, as shown in Equation 21.

$$P_{elec,total,candidates} = (I_{total,demand,candidates} \times V) +$$
$$(I_{total,demand,candidates}{}^2 \times \Omega_{battery}) \tag{21}$$

and then integrated to obtain the electrical energy candidates. Due to the computational limitations, the integration is performed for one second intervals,

and then reset to zero to find the next set of electrical energy candidates. The electric energy consumption candidate's vector is

$$E_{electric,candidates} = [E_{electric}(1) \quad E_{electric}(2) \quad \ldots \quad \ldots \quad \ldots \quad \ldots \quad E_{electric}(n)] \quad (22)$$

where values from each index of the $E_{electric,candidates}$ is the energy consumption by producing a torque value of the corresponding index in $\tau_{motor,candidates}$.

3.2.2.3   Fuel Energy Candidates

A vector of fuel energy consumption that corresponds to each engine torque candidates should be calculated, and then added to the equivalent electrical energy candidates to form a total energy candidates for the controller to evaluate. The $\tau_{engine,candidates}$ with the ω are inputted to the brake specific fuel consumption (BSFC) table to get the instantaneous fuel consumption in kilograms per second for each candidate. These fuel mass flow rates are multiplied by the fuel energy density to find the input fuel power, as shown in equation 1, then all fuel power candidates are integrated over a one second interval to find the equivalent fuel energies. The fuel energy consumption candidates vector is

$$E_{fuel,candidates} = [E_{fuel}(1) \quad E_{fuel}(2) \quad \ldots \quad \ldots \quad \ldots \quad \ldots \quad E_{fuel}(n)] \quad (23)$$

where the each index of the $E_{fuel,candidates}$ is the energy consumption of producing a torque value of the corresponding index in $\tau_{engine,candidates}$.

Equation 24 is used to find the corresponding engine efficiencies if the engine

were to operate at these torque candidates. These efficiencies are then used in the

regulation factor which will be discussed next.

$$\eta_{engine,candidates} = \frac{\tau_{engine,candidates} \times \omega}{P_{fuel}} \tag{24}$$

3.2.2.4   Regulation Factor
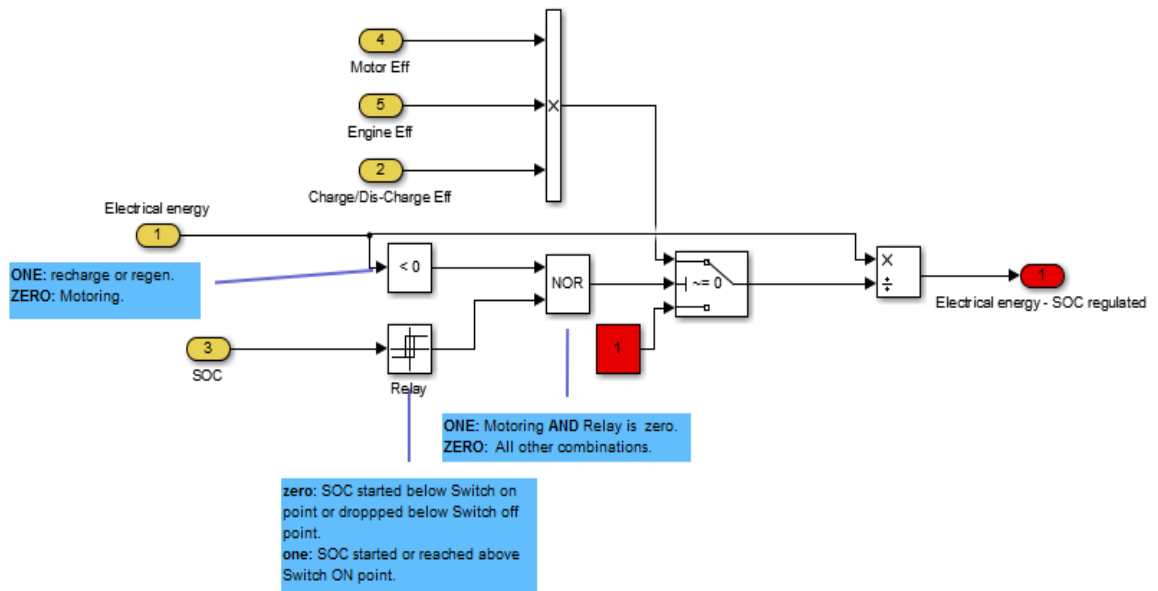
Figure 13: Simulink block diagram of the regulation factor calculations.

A regulation factor is used to adjust the electrical energy candidates in order

to prioritize the engine or the motor for tractive effort, based mainly on the battery

SOC. It also used to determine when to use the motor to regen. The concept of

regulation factor was obtained from [16]. However, they regulated the energies by

random numbers which were claimed as engineering judgments.

This factor either increases (expensive) or decreases (inexpensive) the electric energy for all the candidates based on different conditions. SOC is the main element to decide whether to operate in charge deplete or charge sustain mode. A Relay block is used in Simulink to output a Boolean value which indicates whether the SOC is below or above the limit. The block uses switch ON and OFF limit points to determine the Boolean output. For instance, if the ON and OFF points are set to be 30% and 27% SOC, respectively, the relay outputs zero when the SOC drops below 27%, and maintains this Boolean value until the SOC reaches above 30% and then switches to a value of one.

The regulation factor is equal to one, i.e., it does not change the electrical energy, under the following conditions:

a. $SOC_{relay} = true$ (SOC above minimum threshold): operate in charge deplete mode since the SOC is high.

b. $SOC_{relay} = false$ (SOC below minimum threshold) and $\tau_{demand} < 0$. This means the vehicle is slowing down so the motor is used for regenerative braking.

Moreover, under the conditions described below, the regulation factor increases the electrical energy usage (makes more expensive):

a. $SOC_{relay} = false$ and $E_{electrical} > 0$: the motor is used to provide tractive effort drawing energy from the battery.

b. $SOC_{relay} = false$, $E_{electrical} < 0$ and $\tau_{demand} > 0$: This case is true only when the electrical motor is used as a generator when the energy is coming from the engine while the SOC is below the minimum threshold.

The regulation factor increases the electrical energy by

$$E_{electrical,regulated} = \frac{E_{electrical}}{\eta_{motor} \times \eta_{engine} \times \eta_{charge/discharge}} \qquad (25)$$

This is true assuming that if the engine produces more power than the required for maintaining the desired drive cycle speed and that the extra power is used to increase the SOC, this power will suffer the efficiency losses again when it will be reused for tractive effort in future from the battery. For instance, the process of converting source energy (fuel) into tractive effort at the wheels would require the energy to suffer the following losses due to multiple energy conversions:

1. Engine efficiency (chemical to mechanical)

2. Generating efficiency (mechanical to electrical)

3. Battery charging efficiency (electrical to chemical)

4. Battery discharging efficiency (chemical to electrical)

5. Motoring efficiency (electrical to mechanical)

The actual electric energy consumption value (not regulated) takes the battery discharging and motoring efficiencies into account prior to regulation factor. However, this energy in the battery already suffered engine, generating, and battery charging efficiencies. That is why Equation 25 uses these three efficiencies to regulate to reflect the actual energy usage.

3.2.2.5   Total Energy Consumption

Both fuel energy consumption and SOC regulated electrical energy are added together for each torque combination candidate between the engine and the motor to form the SOC regulated total energy consumption (E_{total}). This total energy consumption takes into consideration all the efficiencies such as battery charge/discharge, battery internal resistance, motor and engine.

3.2.2.6   Emissions

The controller also contains four 2-dimensional look-up tables which contains emissions data for different engine torque and speed combinations. The $\tau_{engine,candidates}$ vector and ω are input into these look-up tables to find the corresponding emission numbers in kilogram per kilometer for Hydrocarbons (HC), Carbon monoxide (CO), Nitrogen oxides (NO$_x$), and Carbon dioxide (CO$_2$). The output of this step is an emission matrix as shown below.

$$Emission = \begin{bmatrix} HC@\tau_{engine}(1) & HC@\tau_{engine}(2) & \dots & \dots & HC@\tau_{engine}(n) \\ CO@\tau_{engine}(1) & CO@\tau_{engine}(2) & \dots & \dots & CO@\tau_{engine}(n) \\ NO_x@\tau_{engine}(1) & NO_x@\tau_{engine}(2) & \dots & \dots & NO_x@\tau_{engine}(n) \\ CO_2@\tau_{engine}(1) & CO_2@\tau_{engine}(2) & \dots & \dots & CO_2@\tau_{engine}(n) \end{bmatrix} \quad (26)$$

3.2.2.7 Normalize All Data

Because the controller has to minimize energy usage and emissions of different pollutants, all of which have different numerical ranges and different units, normalizing is necessary. The normalization of the energy consumption and emission values is done using the equation

$$normalized\ variable\ x = \frac{x - x_{min}}{x_{max} - x_{min}} \tag{27}$$

Equation 27 scales all the data to range between zero and one. Zero corresponds to the minimum value and one corresponds to the maximum value. After normalizing all the total energy consumption and emissions data, the final matrix takes a form of

$$data_{norm} = \begin{bmatrix} E_{total}(1) & E_{total}(2) & \dots & \dots & E_{total}(n) \\ HC@\tau_{engine}(1) & HC@\tau_{engine}(2) & \dots & \dots & HC@\tau_{engine}(n) \\ CO@\tau_{engine}(1) & CO@\tau_{engine}(2) & \dots & \dots & CO@\tau_{engine}(n) \\ NO_x@\tau_{engine}(1) & NO_x@\tau_{engine}(2) & \dots & \dots & NO_x@\tau_{engine}(n) \\ CO_2@\tau_{engine}(1) & CO_2@\tau_{engine}(2) & \dots & \dots & CO_2@\tau_{engine}(n) \end{bmatrix} \tag{28}$$

3.2.2.8 Cost Function and Controller Output

The goals of minimizing the energy consumption and emissions can conflict with each other. This is true because the most energy efficient operating point is not always the same as the operating point with lowest emissions. Also, minimizing emissions of one pollutant by picking a particular operating point might actually increase emission of another. Thus, this controller's design allows the user to pick weights for each of the five characteristics to prioritize the optimization of a particular characteristic. For this purpose, a user defined vector of user weights for

the five characteristics is multiplied by the normalized matrix containing all the energy consumptions and emissions candidates to obtain all data with the desired importance which represents the cost function

$$J = data_{norm,user\ weighted} = k_{user} \times data_{norm} \tag{29}$$

where k_{user} is $1 \times m$, and m is the number of characteristics. Thus the $data_{norm,user\ weighted}$ matrix has dimensions $m \times n$. The index of the lowest point is used in $\tau_{motor,candidates}$ and $\tau_{engine,candidates}$ to find the corresponding torque distribution between the motor and engine. The chosen torque combination, along with the shaft speed are the outputs of the controller to the powertrain.

3.2.3   Real-Time Energy and Emission Minimization Controller (ReTEEM-SS)

This controller is an extension to the main optimization based power flow controller. The process of translating the tractive force request from the driver to torque request is started using three different gear ratios. At each time step, the controller evaluates one lower gear, current gear, and one higher gear. However, if it is at the first or last gear, the possible gears are repeated. The possible gear options take into account the shaft speed limitation based on the vehicle speed. It eliminates the gear option and repeats the current gear in case if:

    a. $\omega_{higher\ Gear} < \omega_{idle}$

    b. $\omega_{lower\ Gear} > \omega_{red\ line}$

A vector of three torque request options is inputted to the modified optimization based controller. It goes through the same calculations but with three times more torque candidates($3n$) since there are three different torque requests. For instance, in the ReTEEM-SS Controller, if $\tau_{motor,candidates}$ vector had 20 candidates, the modified controller will have 60 candidates. The first 20 candidates corresponds to the previous gear, the next 20 candidate corresponds to the current gear, and the last 20 candidates corresponds to the next gear. The controller finds the most efficient candidate, based on the selected user criteria, and then finds the corresponding index. The most efficient candidate index is found using

$$index = \min(data_{norm,user\ weighted}) \tag{30}$$

where $data_{norm,user\ weighted}$ is $1 \times 3n$. It then goes to this index in the vector containing gear numbers for all candidates and selects the value stored at this location as shown below.

$$Gear\ selection = Gear(index) \tag{31}$$

The gear number value is held for one second to improve drivability, and sent as an input to the transmission. This shift logic eliminates the use of traditional shift schedule in the transmission and it bases the shift logic on the defined criteria, such as energy consumption and/or emissions.

Chapter IV

Results

4.1   Simulation Set-up

For each drive cycle three different power flow controllers were compared

using the same vehicle plant models to evaluate the performance of the vehicle. The

three power flow controllers are basic controller, real-time energy and emissions

minimization controller using the standard shift schedule (ReTEEM-SS), and real-

time energy and emissions minimization controller using the developed shift logic

(ReTEEM-SL). To reduce computational time, twenty torque pairs (n =20) were

evaluated at each time-step in both ReTEEM-SS and ReTEEM-SL controllers. Also,

the simulations were run by taking only the energy consumption into consideration

and all emissions were ignored by setting the user defined vector to

$$K_{user} = [1\ 0\ 0\ 0\ 0]$$

4.1.1   Throttle Input to the Transmission

Since the powertrain of the vehicle was modified, the given shift schedule

data from GM for the conventional Camaro is no longer optimized for the hybrid

Camaro with a different ICE and electric motor. For this reason, two different

throttle calculations were used as an input to the shift schedule state flow diagram

in Simulink for the optimization based controller – one using the Equation 2 and the

other equaling zero throttle. An input of zero throttle to the transmission will

eliminate the first variable of the shift schedule state flow, throttle, and the shift

point will depend only on the second variable, vehicle speed. This will result in

upshifts occurring at the lowest vehicle speed threshold which will minimize the

energy consumption. However, the vehicle might not follow the drive cycle if the

powertrain can't deliver the torque request at such low shaft speeds. This scenario

is shown in Figure 14, Figure 15, and Figure 16 in US06 Highway drive cycle using

basic controller with a zero throttle input to the transmission. Since the zero throttle

input will make the transmission shift based on vehicle speed only, the transmission

upshifts as early as possible keeping the RPM very low, as shown in Figure 14.
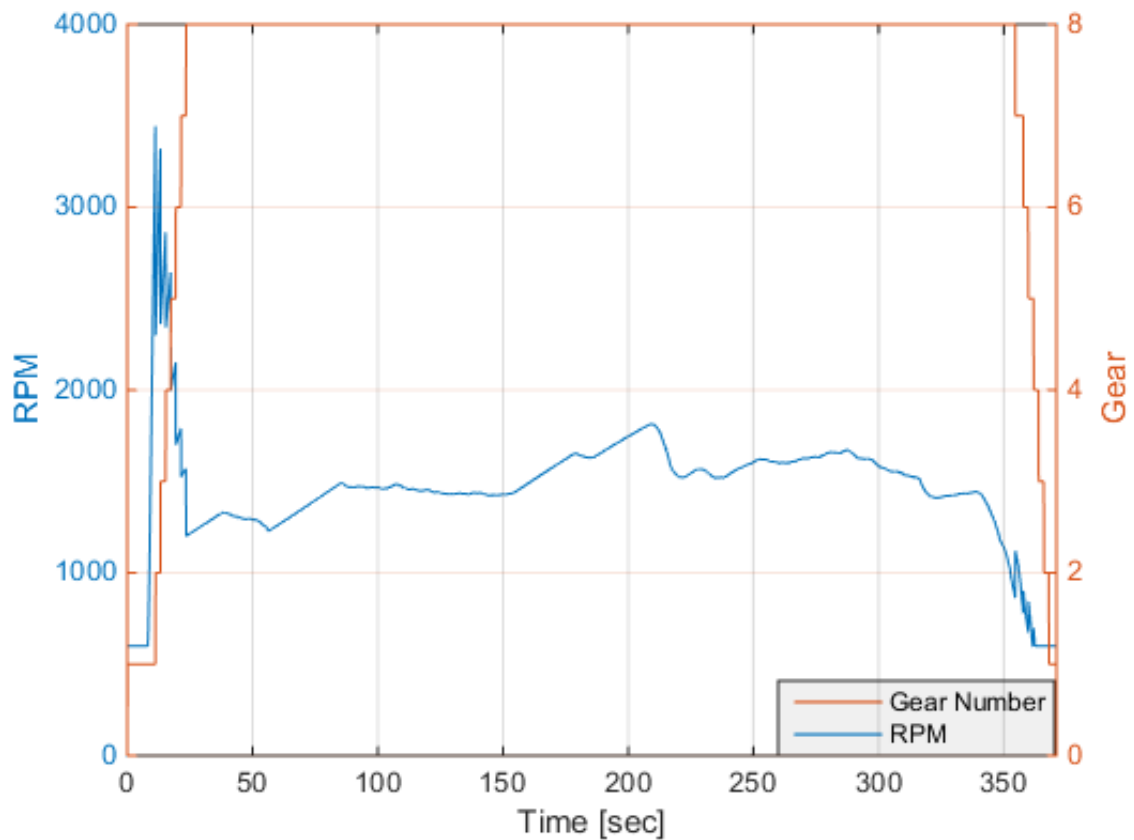
Figure 14: Gear number using US06H drive cycle and Basic controller with a zero throttle input to the transmission.

Figure 15 confirms that the powertrain couldn't meet the desired torque at such low RPM, since the basic controller uses mainly engine only for tractive effort. This resulted for the vehicle not follow the drive cycle, as shown in Figure 16. For this reason the basic controller uses the throttle calculation from Equation 2 as an input to the transmission to determine the shift schedule.
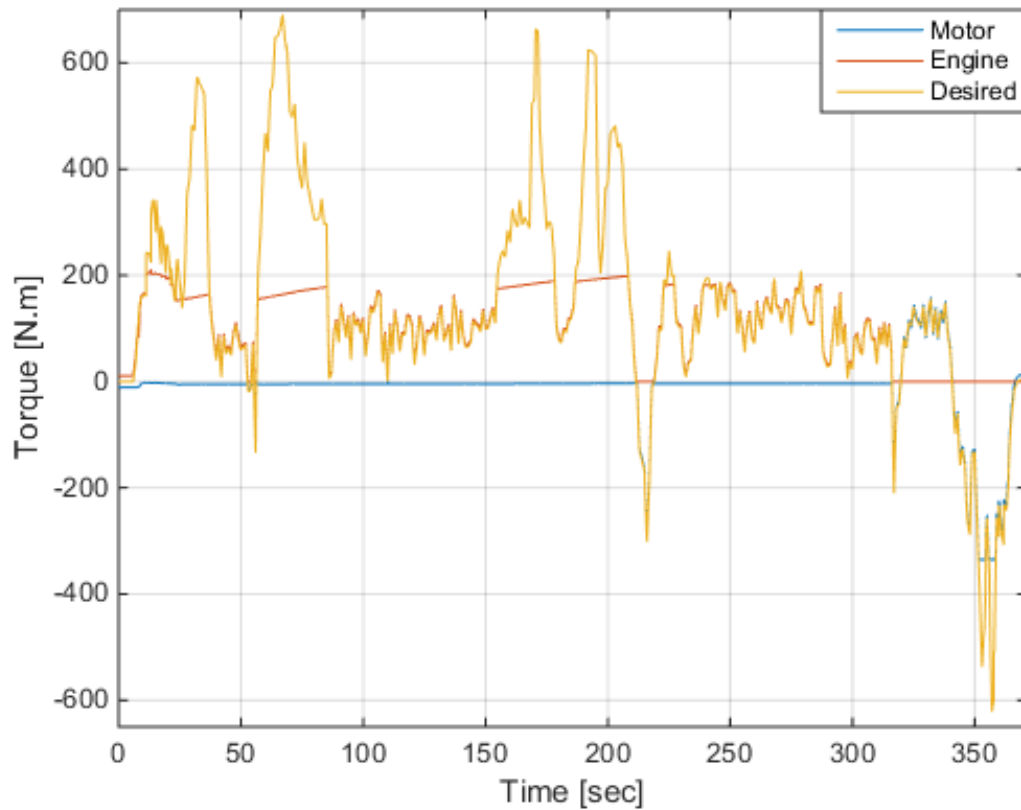
Figure 15: All torques in US06H using Basic controller and zero throttle input to the transmission.
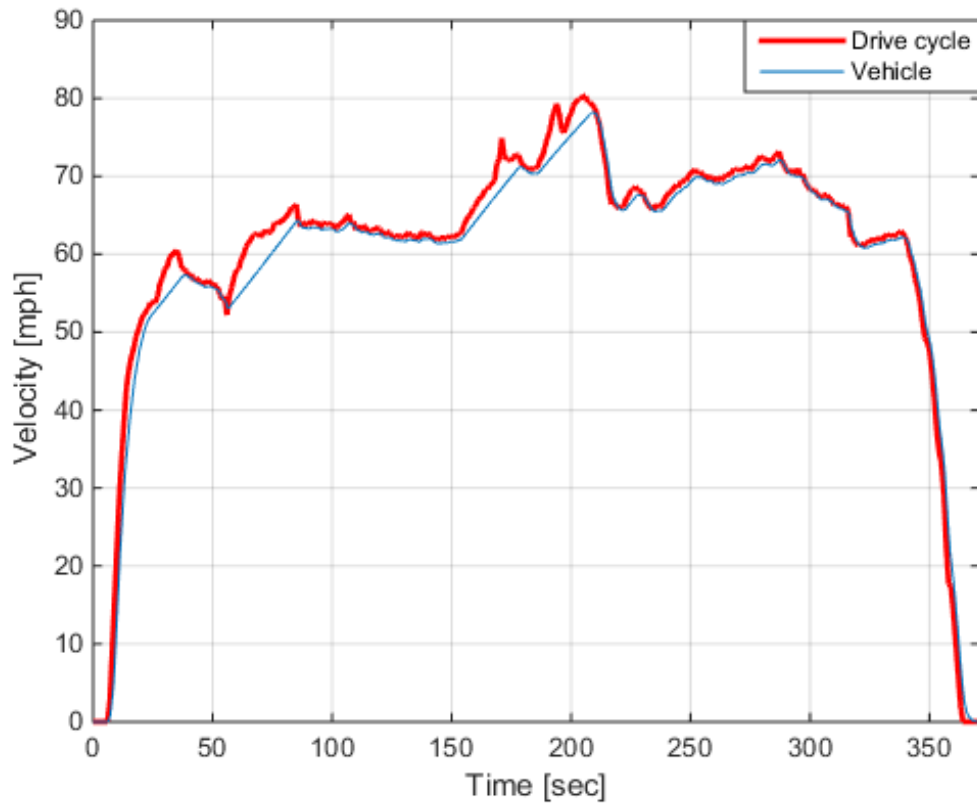
Figure 16: US06H drive cycle and vehicle velocities using basic controller and zero throttle.

4.1.2 Charge Sustain and Response optimization

In CS mode both the ICE and the motor/generator are used to meet the torque demand, giving the different controllers the opportunity to manage the energy differently. All simulations are thus run in this operating mode so that the differences are observable.

Response Optimization Simulink toolbox was used for all the drive cycles to achieve a true CS mode, where the initial and final SOCs are almost identical, as shown in Figure 17.
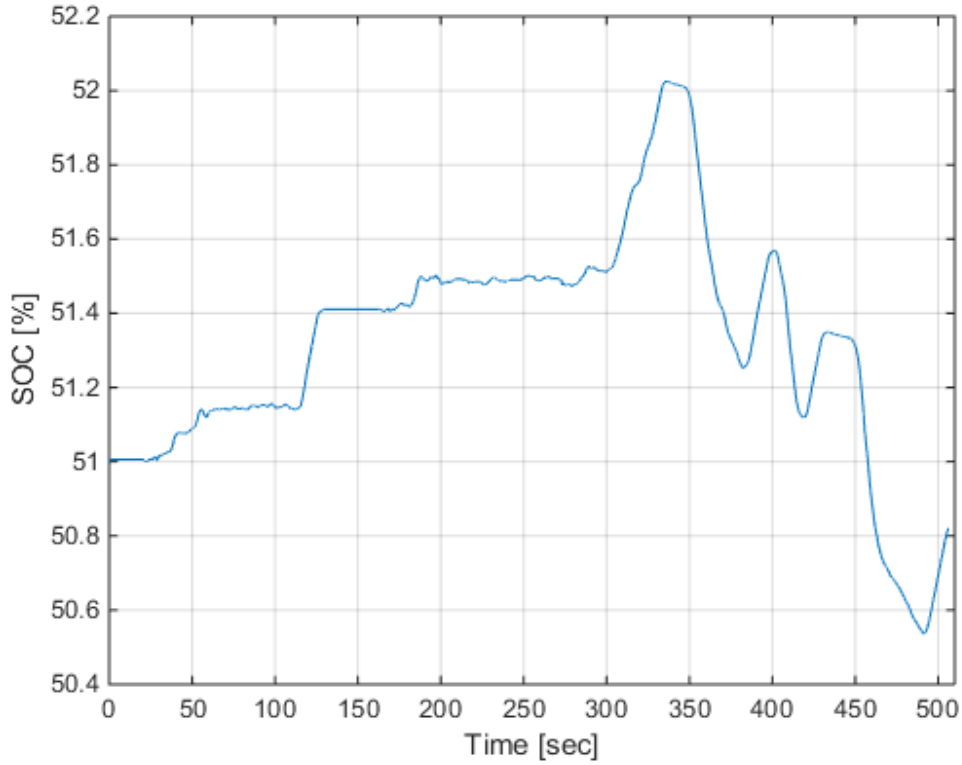
Figure 17: SOC of 505 drive cycle using ReTEEM-SL controller.

Initial SOC was used as the variable to be regulated by the toolbox, and the objective is to minimize the signal that represents the change in SOC. To ensure a true CS mode for energy calculation purposes, some of the drive cycles were repeated in order for the response optimization toolbox to converge. This will not change the result for energy consumption calculations because it is averaged over the total distance traveled. The difference between the initial and final SOCs for all the drive cycles was kept below 1%. However, the equivalent energy consumption resulting from the change in SOC will still be taken into account using equation 30.

$$EC_{\Delta SOC} \left[\frac{W.hr}{km}\right] = \frac{C \times V_{nominal} \times \Delta SOC}{x} \tag{30}$$

where C is the capacity in Ah, $V_{nominal}$ in volts, and x is the total cycle distance in kilometer. It will either be added to or subtracted from the calculated energy consumption to result in final energy consumption value.

4.1.3 Trace Error

To ensure that the vehicle was following all the drive cycles using all controllers, the mean difference between the drive cycle and actual vehicle speed was calculated. These mean differences were kept below 1.3 mph, except for the US06C drive cycle. Since this is the most aggressive drive cycle evaluated, the differences could only be brought down to 3.1 mph. Figure 18 shows that the vehicle follows the US06C drive cycle using all three different controllers.
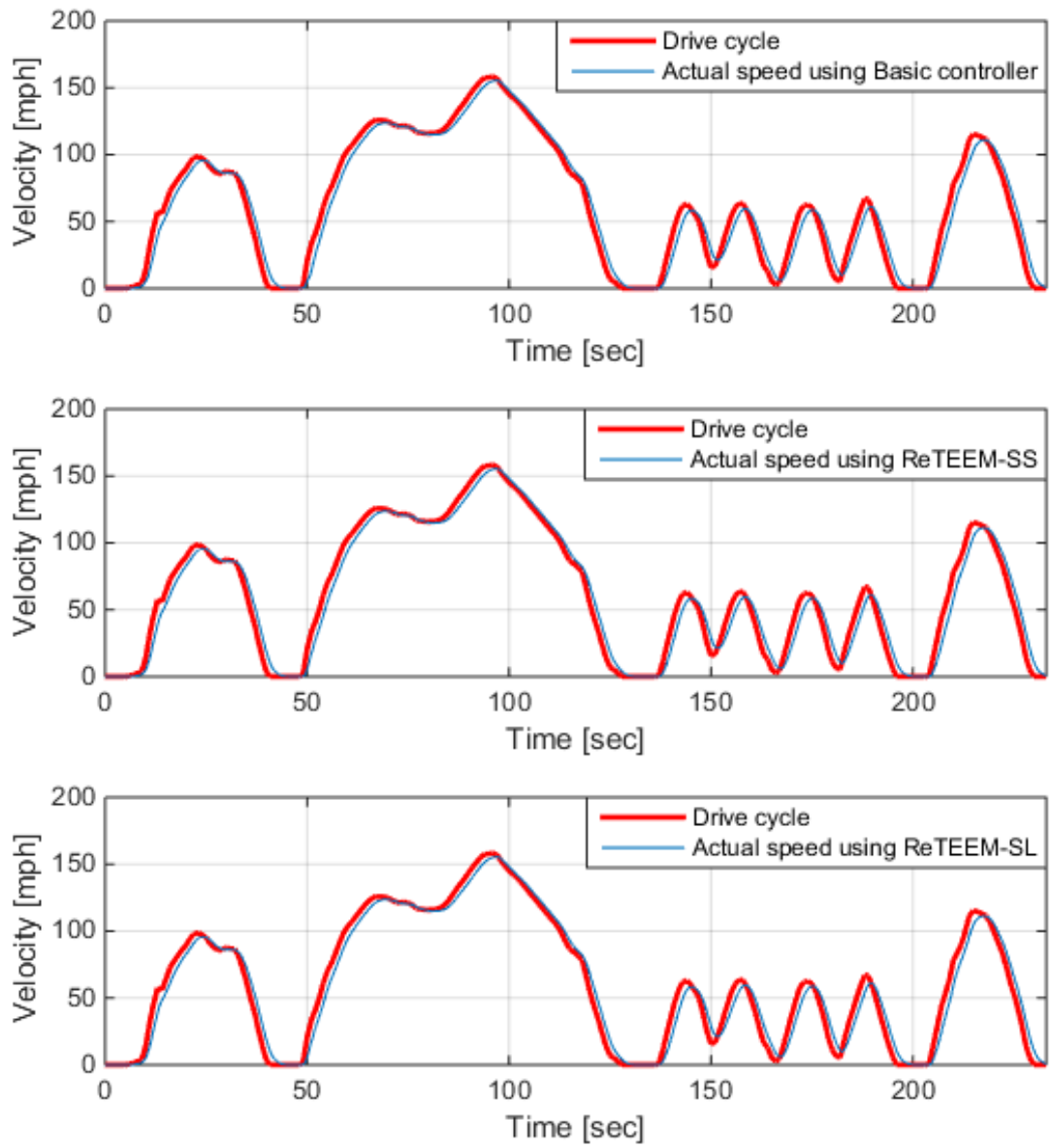
Figure 18: Drive cycle and actual vehicle speed using all three controllers in US06C.

4.2 Varied Torque Apportion from Different Controllers

For illustration purposes, Figure 19, Figure 20 and Figure 21show the desired torque, motor torque, and engine torque for the first 300 seconds of 505 drive cycle for all three different power flow controllers. As shown in Figure 19, the basic controller uses only the engine as the main power source in CS mode, and it uses the motor to generate the auxiliary power and regen from braking.
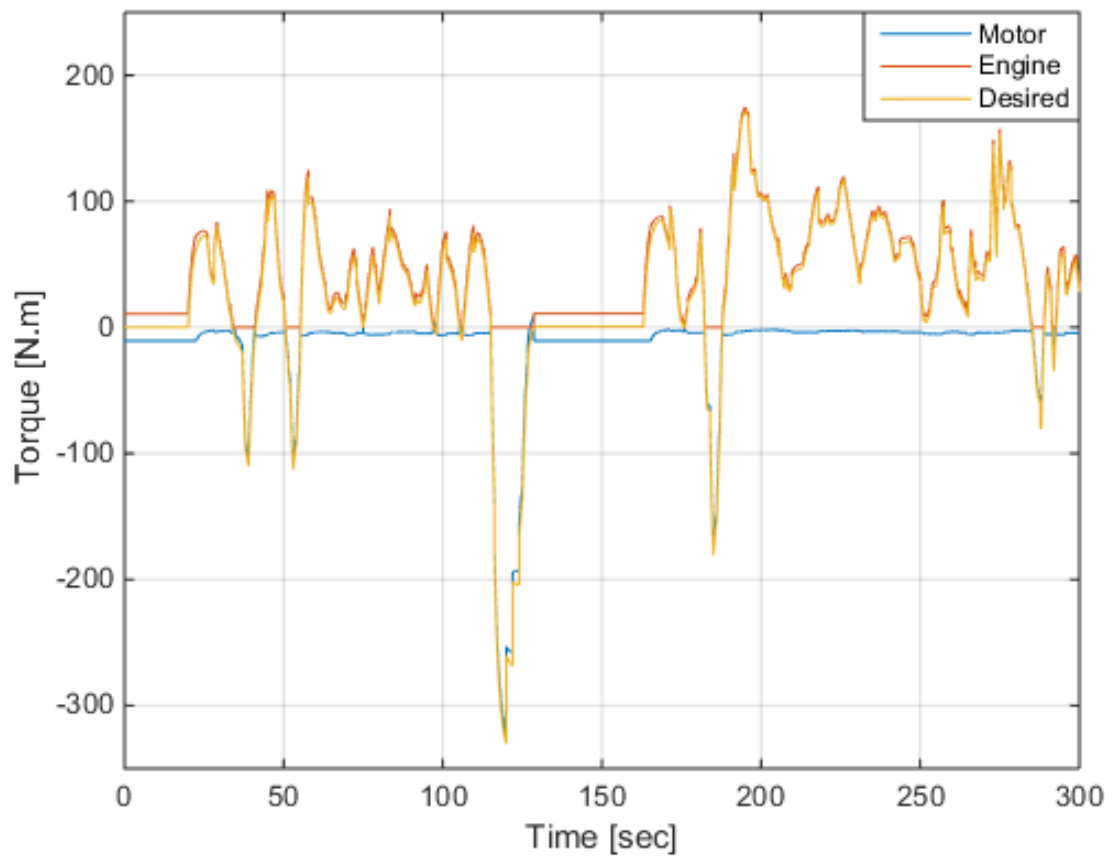
Figure 19: Close-up of all torque requests using basic controller.

Using ReTEEM-SS controller, Figure 20 shows that although the engine is used as the main power source to deliver the desired tractive force, it sometimes uses the motor to assist the engine. Using ReTEEM-SL controller, Figure 21 shows that although the engine is used as the main power source, in some cases the engine makes surplus power in order for the motor to generate electricity to store in the battery. This indicates that there are some torque distribution pairs which are more energy efficient when there is extra load on the engine than the desired tractive force.
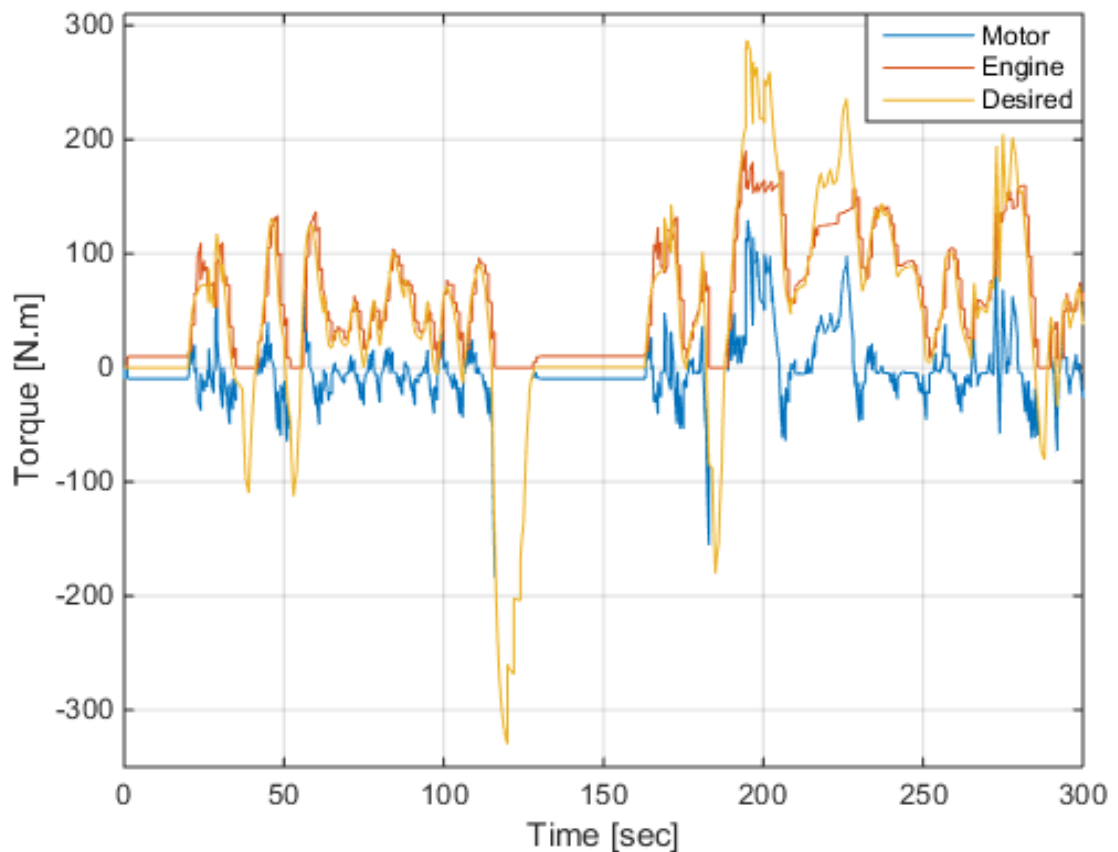
Figure 20: Close-up of all torque requests using ReTEEM-SS controller.
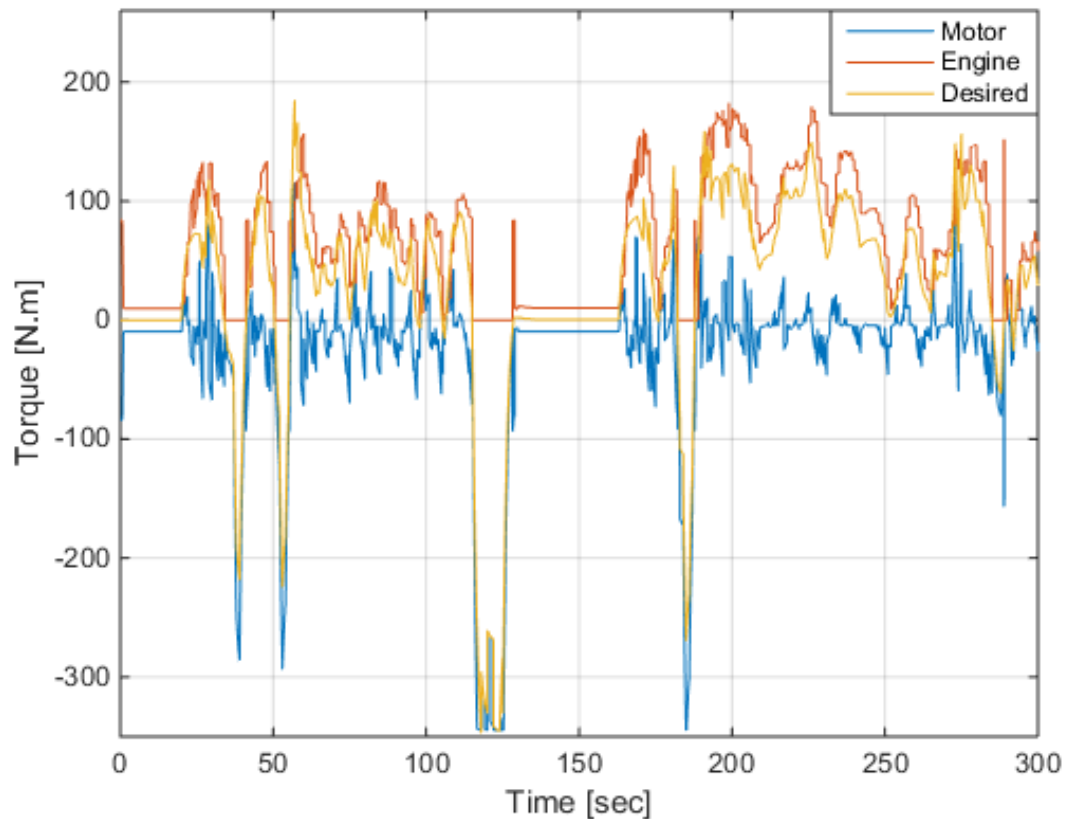
Figure 21: Close-up of all torque requests using ReTEEM-SL controller.

Since all three controllers split the torque differently between the motor and

the ICE, the change in SOC will be different as well, as shown in Figure 22. The

regions with steep positive slopes in the SOC plots are due to braking events of the

505 drive cycle, where the motor functions as a regenerative brake and captures

kinetic energy. All controllers enter charge deplete mode once the SOC reaches the

upper threshold. Then the SOC starts dropping since the controller will prefer to use

the electric motor over the ICE to meet the driver's request. In all simulations, the

SOC upper and lower thresholds were kept close to each other to achieve a true

charge sustain. This allows the vehicle to use the extra gained energy in the battery

from regenerative braking and the engine.
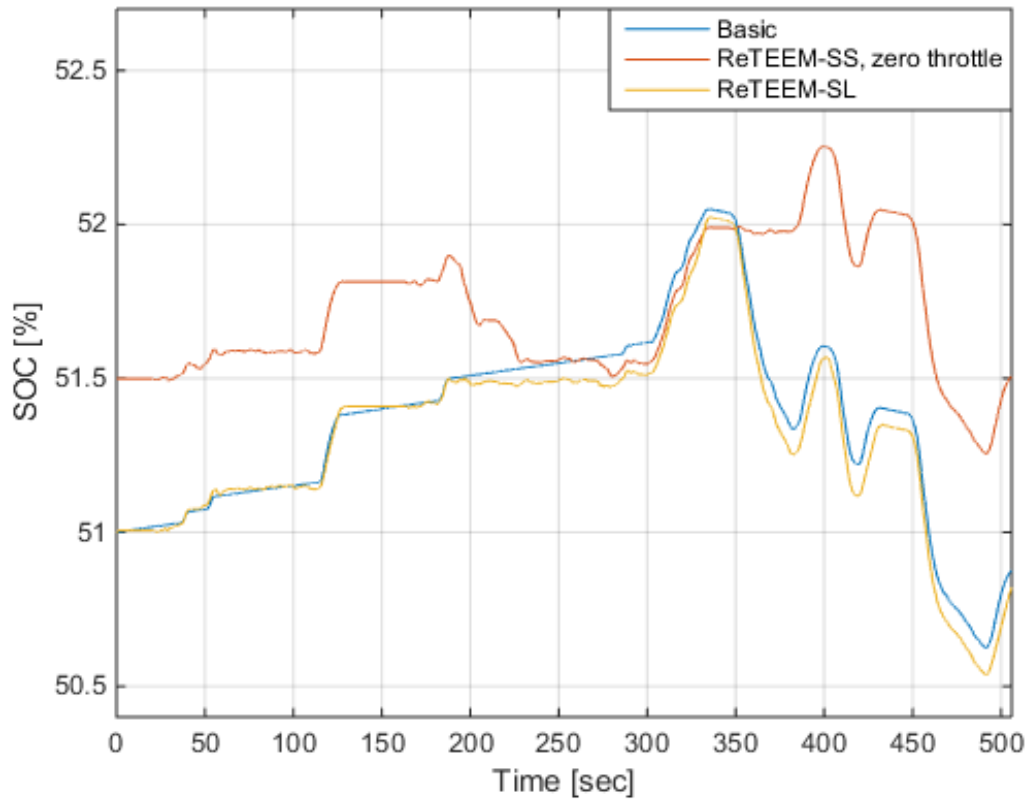
Figure 22: SOC comparison between all the controllers in 505 drive cycle.

4.3   Energy Consumption Comparison

Table 6 , Table 7, Table 10, and Table 11 compare the energy consumption

between the basic controller, ReTEEM-SS controller, ReTEEM-SS controller using

zero throttle, and ReTEEM-SL controller, for all four drive cycles. Since the shift

schedule data is not optimized due to the change in powertrain components, the

optimal energy consumption is expected to be close to the results from using

ReTEEM-SS with zero throttle input. This is because the transmission will shift up to

a higher gear at the lowest possible RPM which will make the engine operate with

low torque outputs. As a result, the controller will demand more torque from the

electric motor to meet the driver's request.

4.3.1 Highway Drive Cycles

Table 6 and Table 7 are energy consumption results for both highway drive cycles, US06 and HWFET. Compared to the basic controller, the ReTEEM-SS controller using zero throttle decreased the total energy consumption by approximately 5.63% in US06H drive cycle and 6.12% in HWFET drive cycle. The total energy consumption using ReTEEM-SL controller is similar to energy consumption using ReTEEM-SS with zero throttle for both highway drive cycles, which indicates that the shift logic decreased the energy without the use of shift schedule.

Table 6: Comparison between all the controllers for US06H drive cycle.

	Basic Controller	ReTEEM-SS	ReTEEM-SS (zero throttle)	ReTEEM-SL
Energy Consumption [Wh/km]	520.1	541.4	488.7	497.7
Delta SOC [%]	0.09	-0.06	-0.20	-0.06
$EC_{\Delta SOC}$ [Wh/km]	-0.9	0.6	1.9	0.6
EC_{final} [Wh/km]	519.1	542.1	490.7	498.3

Table 7: Comparison between all the controllers for HWFET drive cycle.

	Basic Controller	ReTEEM-SS	ReTEEM-SS (zero throttle)	ReTEEM-SL
Energy Consumption [Wh/km]	410.4	424.9	386.7	368.9
Delta SOC [%]	0.32	0.11	0.35	-0.96
$EC_{\Delta SOC}$ [Wh/km]	-3.8	-1.2	-4.3	11.7
EC_{final} [Wh/km]	406.5	423.6	382.4	380.7

One cause of higher energy consumption using basic controller is the limited torque availability at low RPMs, since it uses mainly the ICE to deliver the driver's torque request. Figure 24 shows that using the basic controller the transmission downshifts repetitively to achieve the driver's request. Figure 25 shows the combined electrical energy from the battery and the fuel energy used by the ICE using all three different controllers in HWFET drive cycle. The same figures, gear and energy consumption comparisons, for US06H drive cycle are shown in the Appendix.
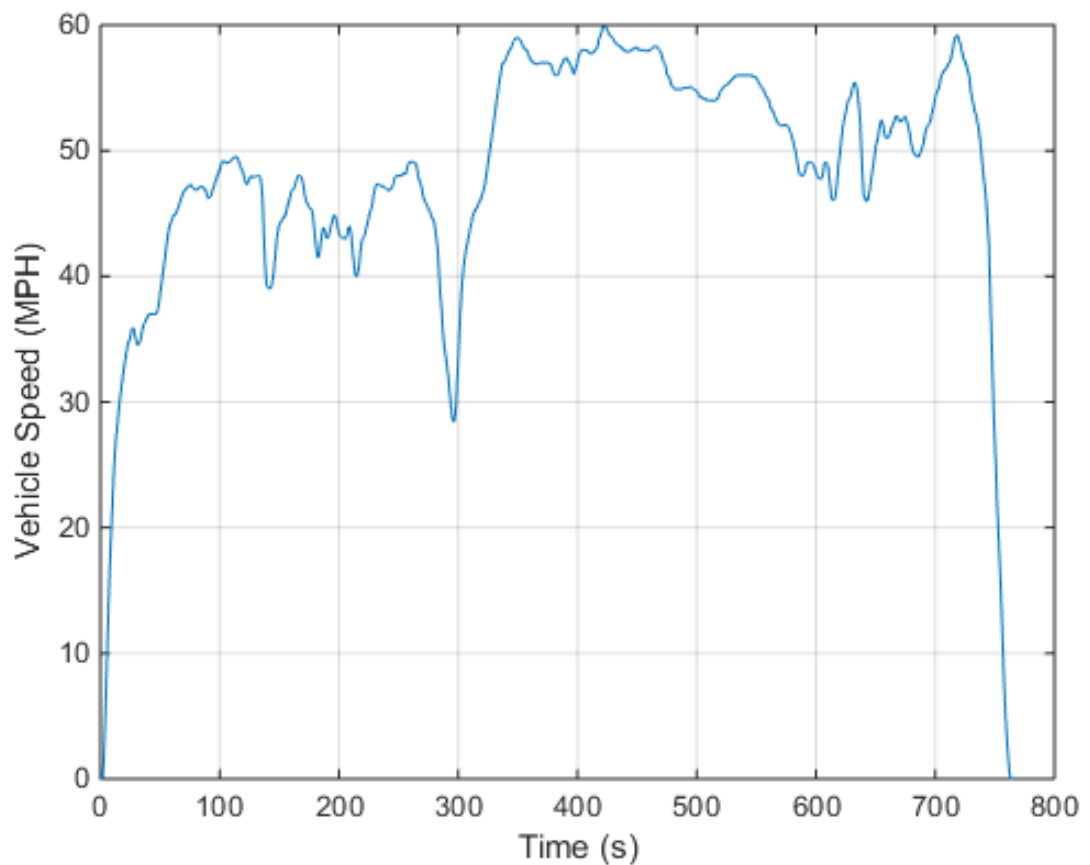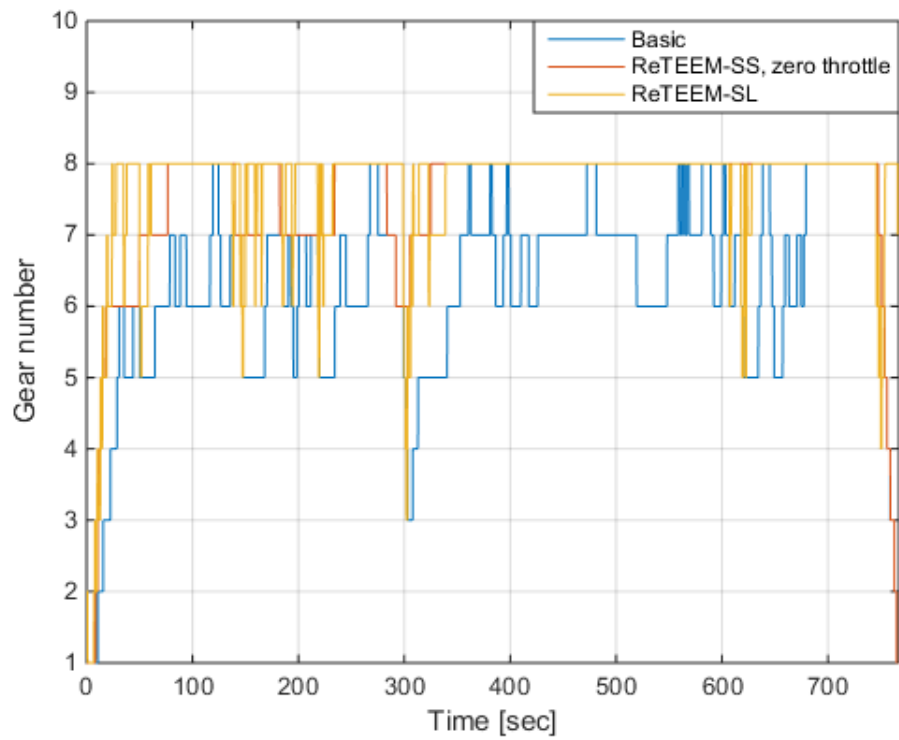

Figure 23: HWFET drive cycle.

Figure 24: Gear number comparison between the three controllers for HWFET drive cycle.
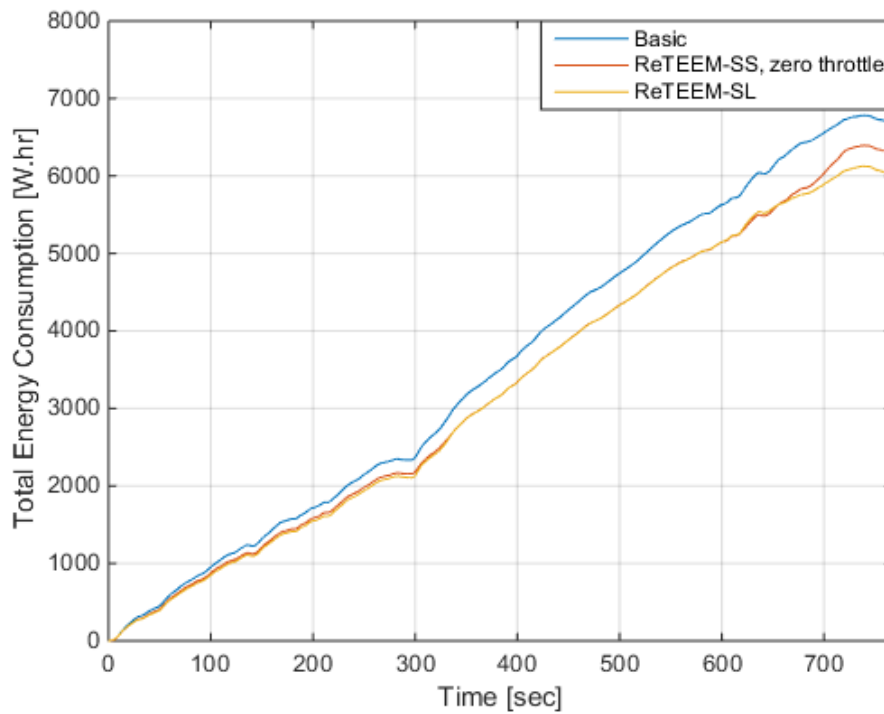

Figure 25: Total energy consumption using all three controllers in HWFET drive cycle.

4.3.1.1 Basic Controller vs. ReTEEM-SS Controller

Each controller distributes the power differently between the power generating components, thus the throttle value differs between controllers. This might cause the vehicle to operate at different gears at the same time in the drive cycle. Different gears and the availability of lesser or more toque in different controllers combine to deviate the vehicle speed differently from the requested speed of the same drive cycle. This causes the Driver model to request different amounts of tractive force from the powertrain. Thus, to compare the basic controller to ReTEEM-SS controller, instantaneous energy consumption data was considered only at times where the difference between the desired tractive force and the output force for the two controllers is within 0.1 N and the vehicle is in the same gear.

Table 8 shows the comparison of instantaneous energy consumption data at a specific time in the HWFET drive cycle between the two controllers. At this time, all the conditions required for comparison are met. The combined instantaneous energy consumption from the engine and the battery using ReTEEM-SS controller is lower than that of basic controller, even though the force request from the driver and the vehicle's operating gear are the same. This is true for 74.8% of the data in the HWFET drive cycle which meets the requirements for comparison – i.e. the required force, output force and the gear number are the same for both controllers at these times. In HWFET drive cycle, only 8.4% of the total data meets the requirements for comparison.

Table 8: Comparing the instantaneous energy using basic and ReTEEM-SS controllers.

	Basic Controller	ReTEEM-SS controller
Time [sec]	121	121
Required force [N]	94.4	94.4
Gear number	8	8
τ_{eng} / τ_{motor} [N.m]	36.3 / -5.7	35.7/-5.2
P_{total} [kW]	12.1	11.9

In the ideal case, the ReTEEM-SS controller should improve the energy consumption at all times when the force request from the driver is the same. However, this is not true since the energy consumption calculation in ReTEEM-SS controller performs integration of instantaneous power over a one second interval because of computational limitations.

The same comparisons were made for US06H drive cycle and showed that 77.0% of the times when the desired force matches and the transmission operates in the same gear, the ReTEEM-SS controller reduced the combined instantaneous energy consumption over the basic controller. The comparable data in US06H drive cycle represents 10.4% of the total data.

4.3.1.2   ReTEEM-SS Controller vs. ReTEEM-SL Controller

Because of differences in driver demand, similar conditions are imposed on the data extracted from simulations using ReTEEM-SS and ReTEEM-SL controllers to make it comparable. At the same time in the drive cycle, the request and output forces still need to be almost identical, but the operating gear has to be different for this comparison. This is because the main difference between the ReTEEM-SS and

ReTEEM-SL controllers is the way they select the operating gear for the vehicle.

Table 9 compares the instantaneous energy consumption data at a specific time

from a simulated HWFET drive cycle when the conditions for comparison are met.

The total output power, from both the engine and the battery, when using ReTEEM-

SL controller is lower than when ReTEEM-SS controller is used. This is true for

90.6% of the data in the HWFET drive cycle which meets the requirements for

comparison – i.e. the required force, output force and gear number are the same for

both controllers at these times. In HWFET drive cycle, only 7.2% of the total data

meets the requirements for comparison.

Table 9: Comparing the instantaneous energy using ReTEEM-SS and ReTEEM-SL controller.

	ReTEEM-SS controller	ReTEEM-SL controller
Time [sec]	43.2	43.2
Required force [N]	350.8	350.8
Gear number	6	8
τ_{eng} and τ_{motor} **[N.m]**	46.6 / -4.5	71.4 / -6.9
P_{total} **[kW]**	21.4	18.7

To increase drivability when using the ReTEEM-SL controller, the operating

gear is held for one second which causes the controller to not always choose the

optimal gear.

The same comparisons were made for US06H drive cycle and showed that

75.4% of the times when the desired force and output force matches, and the

transmission operates in a different gear, the ReTEEM-SL controller reduced the

combined instantaneous energy consumption over the ReTEEM-SS controller. In US06H drive cycle, 4.7% of the total data meets the requirements for comparison.

4.3.2 City Drive Cycles

To evaluate the controllers in city driving styles, simulations were run using 505 and US06C drive cycles. Table 10 and Table 11 show the results of these simulations. Compared to the basic controller, the ReTEEM-SS controller using zero throttle reduced the total energy consumption by 2.78% in 505 drive cycle and 9.60% in US06C drive cycle. The total energy consumption using ReTEEM-SL controller is reduced by 12.57% in 505 drive cycle and 7.76% in US06C drive cycle, compared to the basic controller. This indicates that the shift logic is energy optimized for city drive style as well.

Table 10: Comparison between all the controllers for 505 drive cycle.

	Basic Controller	ReTEEM-SS	ReTEEM-SS (zero throttle)	ReTEEM-SL
Energy Consumption [Wh/km]	440.2	461.3	432.6	385.7
Delta SOC [%]	-0.12	-0.25	0.01	-0.18
$EC_{\Delta SOC}$ [Wh/km]	4.3	8.7	-0.25	6.2
EC_{final} [Wh/km]	444.5	470.1	432.3	392.0

Table 11: Comparison between all the controllers for US06C drive cycle.

	Basic Controller	ReTEEM-SS	ReTEEM-SS (zero throttle)	ReTEEM-SL
Energy Consumption [Wh/km]	699.1	722.9	633.8	650.3
Delta SOC [%]	0.39	0.07	0.31	0.51
$EC_{\Delta SOC}$ [Wh/km]	-9.3742	-1.5863	-7.2303	-12.0535
EC_{final} [Wh/km]	689.8	721.3	626.6	638.3

The comparison between the gears in Figure 27 using basic controller and ReTEEM-SS controller with zero throttle shows that the basic controller usually operates at a lower gear due to the limitation of the desired torque. This is one of the reasons for a higher energy consumption using the basic controller, as shown in Figure 28. The ReTEEM-SL controller always operates at a higher gear than both other controllers, which helps it to have the lowest energy consumption. The significant reduction in energy consumption in 505 drive cycle using ReTEEM-SL over ReTEEM-SS controller is during low vehicle speed operations. From Figure 27, during these operations (340 to 500 seconds), ReTEEM-SL controller upshifts to a higher gear even if the vehicle speed is low, however, the shift schedule using ReTEEM-SS is limited to the vehicle speed thresholds, as discussed in section 3.1.2.4. This gear reduction will allow the ICE and the electric motor to run at lower RPMs which will reduce the energy consumptions. However, due to the aggressive drive cycle and frequent shifting using ReTEEM-SL controller, drivability might be an issue when it is implemented in a real vehicle. The same figures, gear and energy consumption comparisons, for US06C drive cycle are shown in the Appendix.
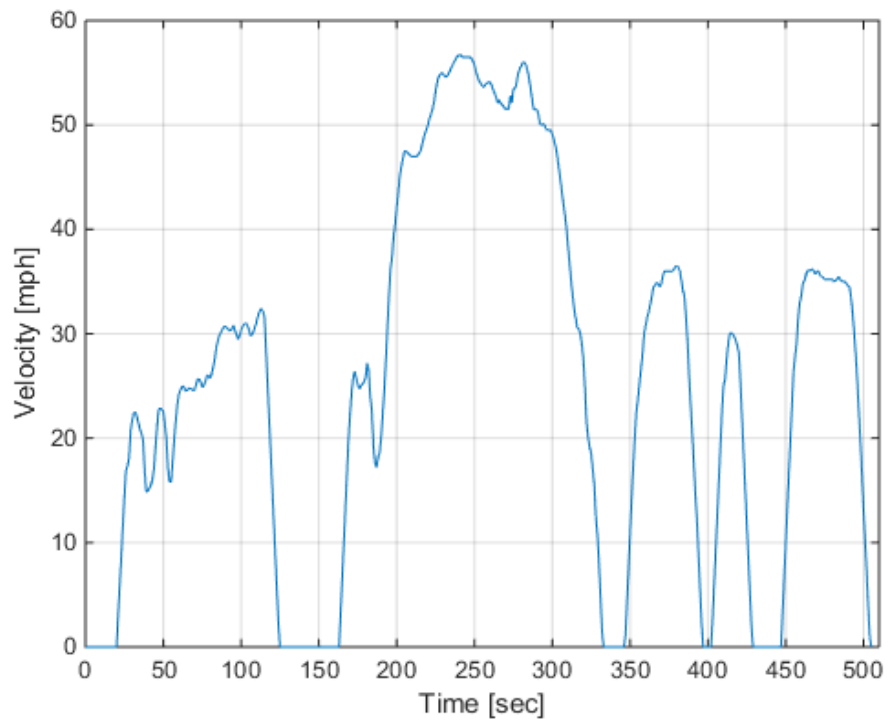
Figure 26: 505 Drive cycle.
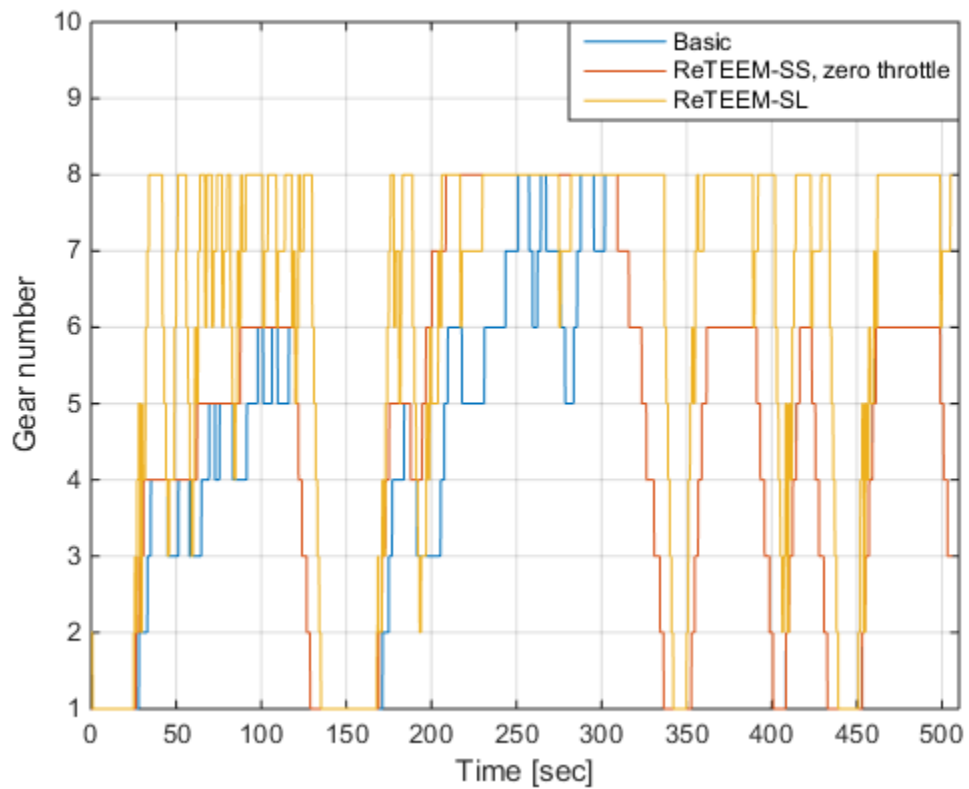
Figure 27: Gear number comparison between the three controllers for 505 drive cycle.
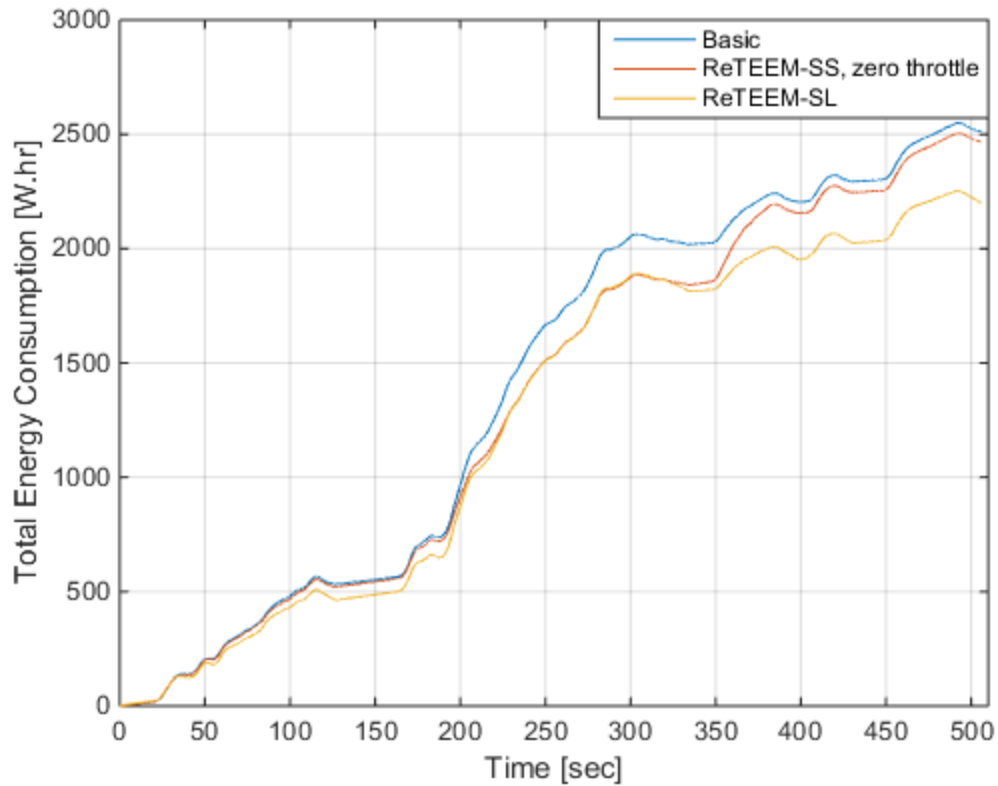
Figure 28: Total energy consumption using all three controllers in 505 drive cycle.

4.3.2.1 Basic Controller vs. ReTEEM-SS Controller

Instantaneous energy consumption data was compared from simulations using basic and ReTEEM-SS controllers for 505 drive cycle. This data had to match the conditions mentioned in Section 4.3.1.1. Results for a specific time are shown in Table 8. The combined instantaneous energy consumption from the engine and the battery using ReTEEM-SS controller is lower than basic controller. This is true for 78.2% of the data when using 505 drive cycle. 20.6% of the total data meets the requirements for comparison.

Table 12: Comparing the instantaneous energy using basic and ReTEEM-SS controllers.

	Basic Controller	ReTEEM-SS controller
Time [sec]	252	252
Required force [N]	19.4	19.4
Gear number	8	8
τ_{eng} and τ_{motor} [N.m]	8.6 / -5.1	8.8 / -5.2
P_{total} [kW]	8.7	7.2

The same comparisons were made for US06C drive cycle and showed that the ReTEEM-SS controller is better than the basic controller for 75.6% of the comparable data. The comparable data represents 16.3% of the total data.

4.3.2.2   ReTEEM-SS Controller vs. ReTEEM-SL Controller

Instantaneous energy consumption data was compared from simulations using ReTEEM-SS and ReTEEM-SL controllers for 505 drive cycle. This data had to match the conditions mentioned in Section 4.3.1.2. Results for a specific time are shown in Table 8. The combined instantaneous energy consumption from the engine and the battery using ReTEEM-SL controller is lower than ReTEEM-SS controller. This is true for 89.0% of the data when using 505 drive cycle. The comparable data in 505 drive cycle represents 20.6% of the total data.

Table 13: Comparing the instantaneous energy using ReTEEM-SS and ReTEEM-SL controller.

	ReTEEM-SS controller	ReTEEM-SL controller
Time [sec]	64.7	64.7
Required force [N]	189.9	189.9
Gear number	5	8
τ_{eng} and τ_{motor} [N.m]	40.8 / -23.0	44.7 / -9.7
P_{total} [kW]	15.0	10.6

The same comparisons were made for US06C drive cycle and showed that the

ReTEEM-SL controller is better than the ReTEEM-SS controller for 87.0% of the

comparable data, which it represents 16.0% of the total data.

Chapter V

Discussions, Future work, and Conclusions

5.1   Discussions

The results for both optimization based power flow controllers using shift schedule and shift logic show a reduction in energy consumption when compared to the basic controller. Since the ReTEEM-SS controller uses the shift schedule, experimental tests need to be carried out to obtain the shifting thresholds. Therefore in simulation it is harder to evaluate the performance of the same vehicle using different components in the powertrain or different parallel powertrain architectures.

To overcome this issue, ReTEEM-SL controller uses shift logic to select the gear which eliminates the use of shift schedule, therefore no experimental tests need to be carried out. Also, the controller can be used to develop a shift schedule without experimental data. However, since the ReTEEM-SL controller evaluates all the torque candidates for three different gears at each time step, it might be computationally more expensive when the controller is implemented in the actual vehicle.

One main variable that can be calculated differently and affect the performance of the vehicle significantly is the throttle. As shown in Table 6 through Table 11, the energy consumption of the vehicle changes considerably when using the same controller but a different throttle input. This means that using ReTEEM-SS

controller, the energy consumption can be further reduced by calculating the throttle differently.

One of the main advantages of both ReTEEM-SS and ReTEEM-SL controllers is the flexibility to evaluate different components in the parallel architecture powertrain without any modification to the controller. The controller can be applied to any powertrain architecture that splits the torque between different power generating components at the same shaft speed. In addition, the developed controller is capable of taking other factors, such as temperature, besides energy consumption and emissions into consideration by adding rows to the matrix $data_{norm,user\ weighted}$.

5.2 Future Work

5.2.1 Implementation and Validation

The optimization based controller has the potential to be effective and implementable on the actual EcoCAR 3 vehicle. First, the controller needs to run with fix time-step and then check if it can be implemented on the controller hardware. Then the controller needs to be slightly modified to take the actual component statuses as inputs. For example, the controller needs to know the actual status of the engine due to a fault mode, low fuel, or overheating, in order to appropriately split the torque between the power generating components. Another input the controller will need is the actual status of the clutches to determine what components can be used to achieve the driver's torque request.

In the actual vehicle, the driver can choose between different driving modes such as sport and economy. This feature needs to be added to the controller so that if the driver selects power mode, all the power generating components run at their peak without taking any energy consumption and emissions into consideration.

Once the controller is ready to be used in the actual vehicle, the next step is to carry out tests and collect data to compare with the Simulink model. This can be done by driving the actual vehicle and collect all the necessary data, and then input the actual velocity profile to the Simulink model and compare the results.

5.2.2 Predictive Control Strategy

One additional feature that can be added to this controller to be more energy efficient is the use of GPS to predict the future driving pattern. For example, it is

more energy efficient to depend on the electric motor and drop the battery's SOC below the minimum threshold if the vehicle is close to the destination and the battery can be recharged. The selection of gears can also be modified to suit the upcoming road conditions and traffic patterns.

5.2.3 Three-way Split

The hybrid Camaro that the EcoEagles team is building has two electric motors and ICE. The controller needs to be modified to split the torque between all three power generating components to possibly further optimize energy consumption and emissions.

5.2.4 Emissions

The Methodology section in this thesis explains how the controller will take emissions into consideration, but it wasn't evaluated due to lack of reliable data. To verify that the controller reduces the emissions, simulations should be run to compare with the basic controller when reliable emissions data is available.

5.2.5 Shift Schedule Mapping

Shift maps can be generated using the ReTEEM-SL controller. This can be done by using adaptive look up tables to generate shift maps that reduces the energy consumption and emissions.

5.3   Conclusion

The reduction in energy consumption of the HEV using the new optimization based controller has been shown, with a potential of reducing emissions if accurate data were available. Compared to the basic power flow controller, the real-time energy and emission minimization controller (ReTEEM-SS) reduced the energy consumption by approximately 6.2% in city driving style and 5.4% in highway driving style. This was using zero throttle as an input to the shift schedule which will result in upshifting as soon as possible, therefore minimizing the energy consumption. The optimization based controller was further modified to replace the shift schedule with a shift logic. The shift schedule is tuned experimentally by driving the vehicle in different conditions and eliminating this makes evaluating different components on the vehicle's powertrain easier. The real-time energy and emission consumption controller using shift logic (ReTEEM-SL) reduced the energy consumption by 10.2% in city drive cycles and 5.3% in highway drive cycles, when compared to the basic controller.

References

[1] B. M. Baumann, "Mechatronic design and control of hybrid electric vehicles," *IEEE/ASME Transactions on Mechatronics*, vol. 5, no. 1, pp. 58-72, 2000.

[2] Tao Zhao, "Simulation of Fuzzy Optimal Control Strategy on a Parallel Hybrid Electrical Vehicle," *Intelligent Control and Automation,* vol. 2, pp. 8306-8310, 2006.

[3] S. Adhikari, "An Online Power-Balancing Strategy for a Parallel Hybrid Electric Vehicle Assisted by an Integrated Starter Generator," *IEEE Transactions on Vehicular Technology,* vol. 59, no. 6, pp. 2689 - 2699, 2010.

[4] A. Sciarretta, "Optimal control of parallel hybrid electric vehicles," *IEEE Transactions on Control Systems Technology,* vol. 12, no. 3, pp. 352-363, 2004.

[5] Y. Zhao, "Simulation and fuzzy logic analysis on an Off-road HEV," *Consumer Electronics, Communications and Networks (CECNet),* pp. 710-714, 2011.

[6] F. R. Salmasi, "Control Strategies for Hybrid Electric Vehicles: Evolution, Classification, Comparison, and Future Trends," *IEEE Transactions on Vehicular Technology,* vol. 56, no. 5, pp. 2393-2404, 2007.

[7] C. Ma, "Comparative study on power characteristics and control strategies for plug-in HEV," *Vehicle Power and Propulsion Conference (VPPC),* pp. 1-6, 2011.

[8] C. C. Chan, "Power flow control," in *Modern Electric Vehicle Technology*, Oxford University Press, 2001, p. 55.

[9] H.-D. Lee, "Fuzzy-logic-based torque control strategy for parallel-type hybrid electric vehicle," *IEEE Transactions on Industrial Electronics,* vol. 45, no. 4, pp. 625-632, 1998.

[10] W. Yifeng, "Energy management system based on fuzzy control approach for hybrid electric vehicle," *Control and Decision Conference,* pp. 3382-3386, 2009.

[11] A. Ahmed, "Control and analysis of regenerative power distribution on electrical variable transmission using fuzzy logic on HEV system," *Electrical Machines and Systems (ICEMS),* pp. 1-6, 2011.

[12] A. A. Abdelsalam, "Fuzzy logic global power management strategy for HEV based on permanent magnet-dual mechanical port machine," *Power Electronics and Motion Control Conference (IPEMC),* vol. 2, pp. 859-866, 2012.

[13] Y. Gaoua, "Energy management using fuzzy logic, on HEV," *Electric Vehicle Symposium and Exhibition (EVS27),* pp. 1-7, 2013.

[14] M. Ehsani, Y. Gao and A. Emadi, Modern Electric, Hybrid Electric, and Fuel Cell Vehicles, 2nd ed., R. Muhammed H, Ed., Boca Raton, Florida: Taylor and Francis Group, 2000, pp. 293-294.

[15] A. Khajepour, S. Fallah and A. Goodarzi, Electric and Hybrid Vehicles, Chichester: Wiley, 2014, p. 337.

[16] V. Johnson, "HEV Control Strategy for Real-Time Optimization of Fuel Economy and Emissions," 2000.

[17] T. Leroy, "Towards real-time optimal energy management of HEV powertrains using stochastic dynamic programming," *Vehicle Power and Propulsion Conference (VPPC),* pp. 383-388, 2012.

[18] J. Jeong, "Analysis of fuel economy and battery life depending on the types of HEV using dynamic programming," *Electric Vehicle Symposium and Exhibition (EVS27),* pp. 1-5, 2013.

[19] Y. b. Yu, "Control strategy optimization research using Dynamic Programming method for Synergic Electric System on HEV," *Intelligent Vehicles Symposium,* pp. 770-774, 2009.

[20] C. Musardo and B. Staccia, "Energy management strategies for hybrid electric vehicles," Milan, 2004.

[21] Q. Gong, "Optimal power management of plug-in HEV with intelligent transportation system," *Advanced intelligent mechatronics,* pp. 1-6, 2007.

[22] M. H. Hajimiri, "A Fuzzy Energy Management Strategy for Series Hybrid Electric Vehicle with Predictive Control and Durability Extension of the Battery," *Electric and Hybrid Vehicles,* pp. 1-5, 2006.

[23] S. Ichikawa, "Novel energy management system for hybrid electric vehicles utilizing car navigation over a commuting route," *Intelligent Vehicles Symposium,* pp. 161-166, 2004.

[24] "Dynamometer Drive Schedules," 24 March 2016. [Online]. Available: https://www.epa.gov/vehicle-and-fuel-emissions-testing/dynamometer-drive-schedules.

[25] Y. Meng, R. Gulati, A. Karmustaji, H. Khalifi and A. Szechy, "Modeling and Control Strategy Development of a Parallel-Series Plug-in Hybrid Electric Vehicle," EcoCAR, Daytona Beach, 2015.

[26] H. Khalifi, "Hybrid Electric Power System Validation through Parameter Optimization," M.S Thesis, ERAU, Daytona Beach, 2015.

[27] GM, "gmauthority," General Motors, [Online]. Available: http://gmauthority.com/blog/gm/gm-transmissions/m5u/#tab-2. [Accessed 13 4 2016].

[28] B. d. Jager, T. v. Keulen and J. Kessels, Optimal Control of Hybrid Vehicles, Springer, London, 2013, pp. 39-45.
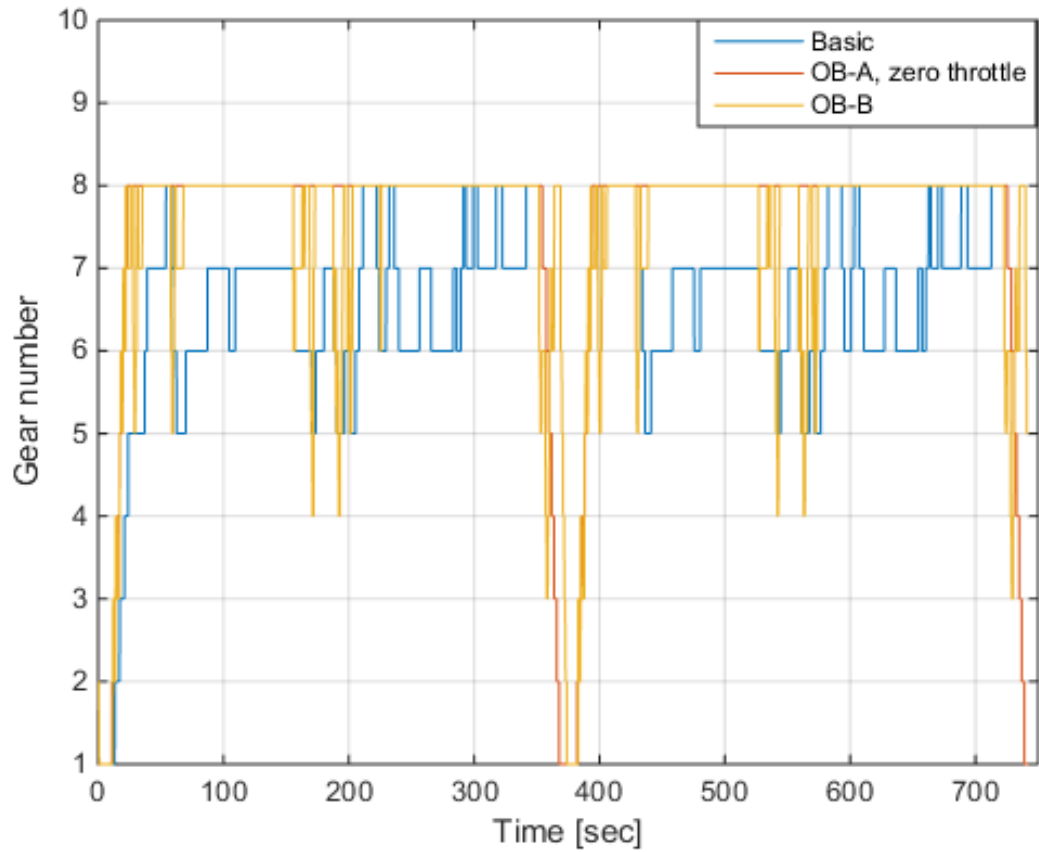
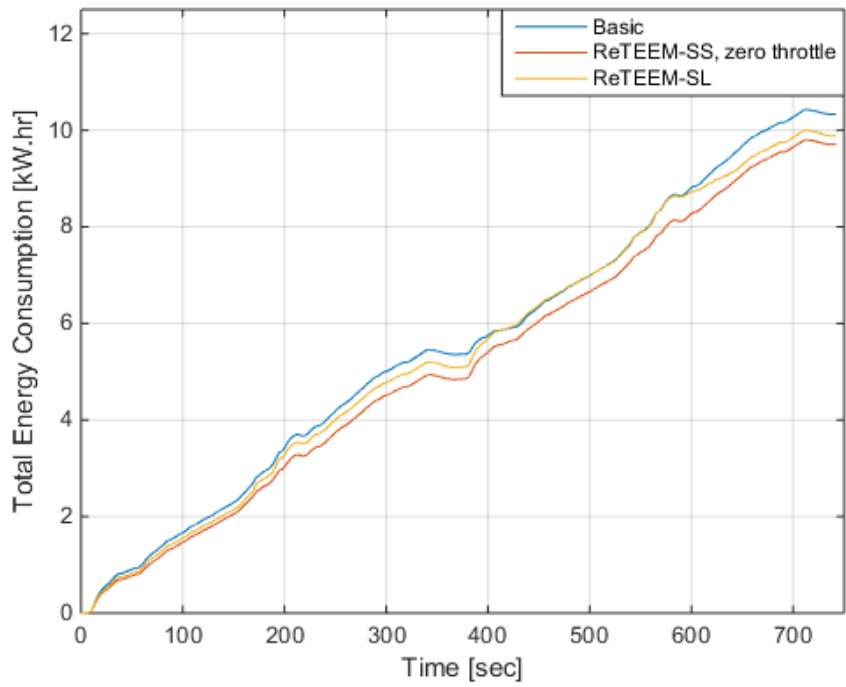Figure 29: Gear number comparison between the three controllers for US06H drive cycle.

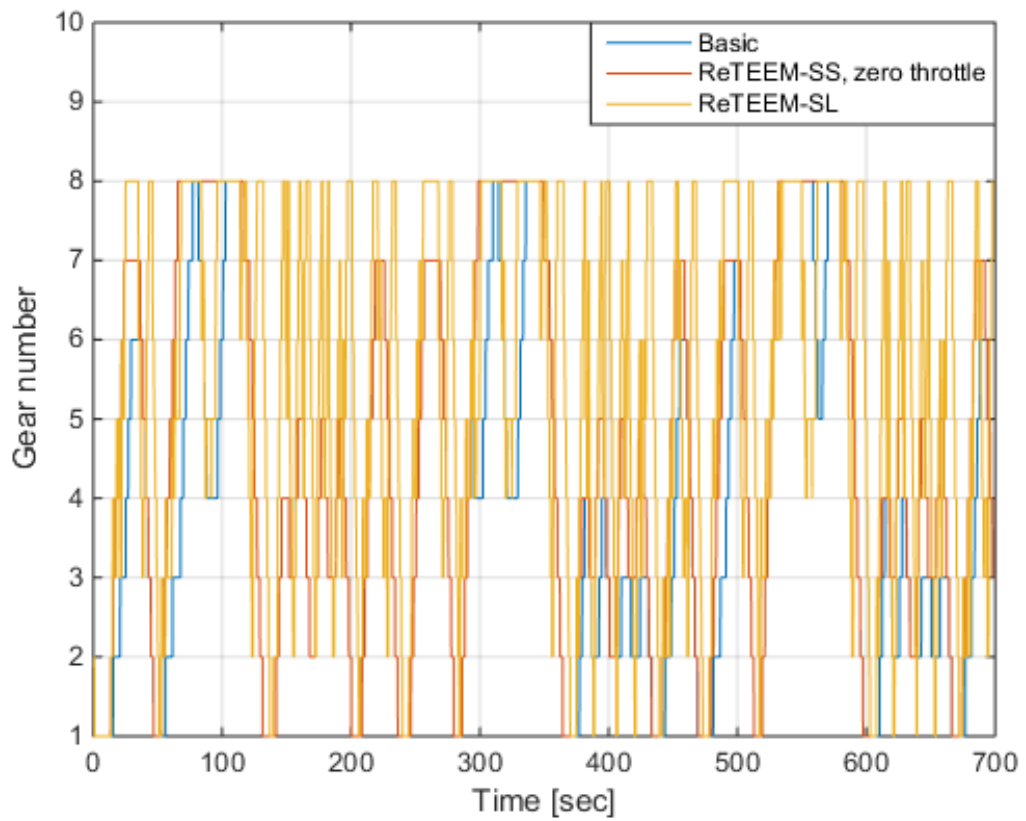Figure 30: Total energy consumption using all three controllers in US06H drive cycle.

Figure 31: Gear number comparison between the three controllers for US06C drive cycle.
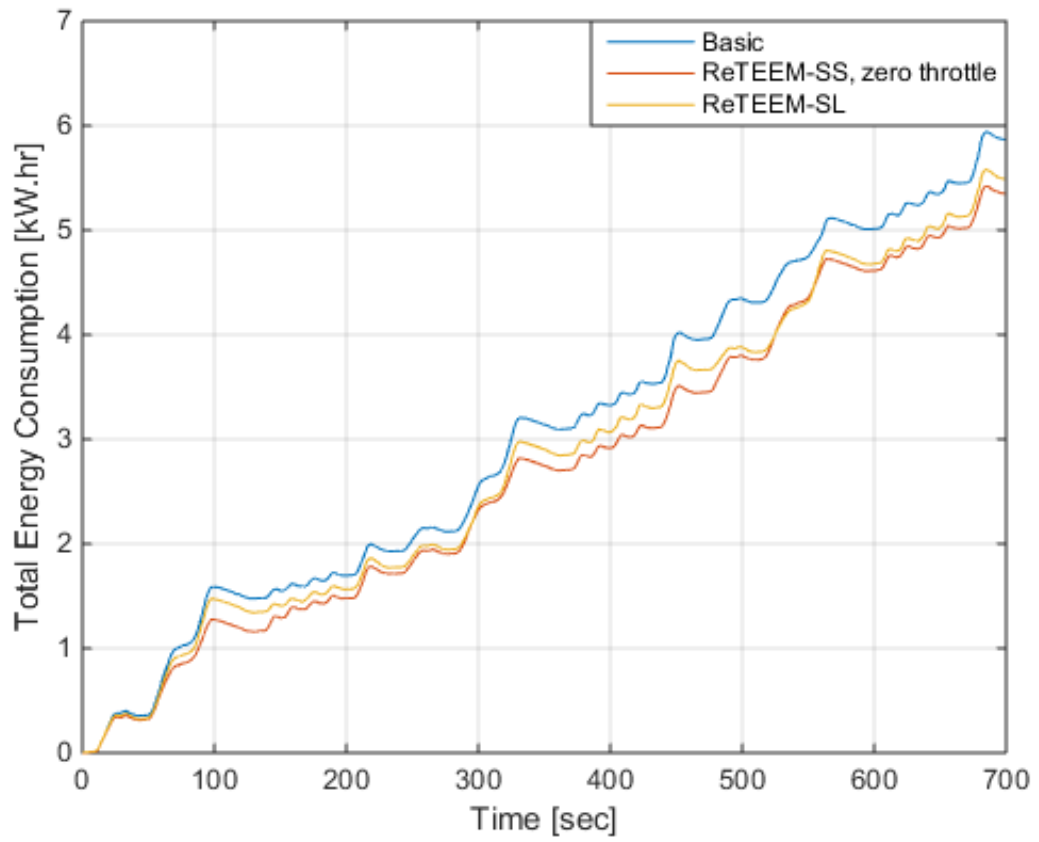
Figure 32: Total energy consumption using all three controllers in US06C drive cycle.